GEOLOGIC AND GEOPHYSICAL MAPS AND VOLCANIC HISTORY OF THE KELTON PASS SE AND MONUMENT PEAK SW QUADRANGLES, BOX ELDER COUNTY, UTAH

by Tracey J. Felger, David M. Miller, Victoria E. Langenheim, and Robert J. Fleck

MISCELLANEOUS PUBLICATION 16-1DM
UTAH GEOLOGICAL SURVEY
a division of
UTAH DEPARTMENT OF NATURAL RESOURCES
in cooperation with
U.S. Department of the Interior
U.S. Geological Survey
2016

GEOLOGIC AND GEOPHYSICAL MAPS AND VOLCANIC HISTORY OF THE KELTON PASS SE AND MONUMENT PEAK SW QUADRANGLES, BOX ELDER COUNTY, UTAH

by Tracey J. Felger [1], David M. Miller [2], Victoria E. Langenheim [2], and Robert J. Fleck [2]

[1] U.S. Geological Survey, 2255 N. Gemini Drive, MS-7420, Flagstaff, AZ 86001
[2] U.S. Geological Survey, 345 Middlefield Road, MS-973, Menlo Park, CA 94025

GEOLOGIC MAP 1:24,000 SCALE

Cover photo: *South end of the Wildcat Hills. The Provo shoreline (Lake Bonneville) forms a well-defined wave-cut platform in the Pleistocene Rhyolite of Wildcat Hills (2.3 Ma). Light colored outcrops at base of slope are lacustrine deposits from Lake Bonneville overlying air fall tuff and tuffaceous sedimentary rocks of the Miocene Salt Lake Formation.*

ISBN: 978-1-55791-919-9

UTAH DNR GEOLOGICAL SURVEY

USGS science for a changing world

MISCELLANEOUS PUBLICATION 16-1DM
UTAH GEOLOGICAL SURVEY
a division of
UTAH DEPARTMENT OF NATURAL RESOURCES
in cooperation with
U.S. Department of the Interior
U.S. Geological Survey
2016

STATE OF UTAH
Gary R. Herbert, Governor

DEPARTMENT OF NATURAL RESOURCES
Michael Styler, Executive Director

UTAH GEOLOGICAL SURVEY
Richard G. Allis, Director

PUBLICATIONS
contact
Natural Resources Map & Bookstore
1594 W. North Temple
Salt Lake City, UT 84114
telephone: 801-537-3320
toll-free: 1-888-UTAH MAP
website: mapstore.utah.gov
email: geostore@utah.gov

UTAH GEOLOGICAL SURVEY
contact
1594 W. North Temple, Suite 3110
Salt Lake City, UT 84114
telephone: 801-537-3300
website: geology.utah.gov

This geologic map was funded by the U.S. Geological Survey. The views and conclusions contained in this document are those of the authors and should not be interpreted as necessarily representing the official policies, either expressed or implied, of the U.S. Government.

CONTENTS

FIGURES

TABLES

PLATES

GEOLOGIC AND GEOPHYSICAL MAPS AND VOLCANIC HISTORY OF THE KELTON PASS SE AND MONUMENT PEAK SW QUADRANGLES, BOX ELDER COUNTY, UTAH

by Tracey J. Felger, David M. Miller, Victoria E. Langenheim, and Robert J. Fleck

INTRODUCTION

The Kelton Pass SE and Monument Peak SW 7.5′ quadrangles are located in Box Elder County, northwestern Utah (figure 1; plate 1). The northern boundary of the map area is 8.5 miles (13.7 km) south of the Utah-Idaho border, and the southern boundary reaches the edge of mud flats at the north end of Great Salt Lake. Elevations range from 4218 feet (1286 m) along the mud flats to 5078 feet (1548 m) in the Wildcat Hills. Deep Creek forms a prominent drainage between the Wildcat Hills and Cedar Hill. The closest towns are the ranching communities of Snowville, Utah (10 miles [16 km] to the northeast) (figure 1), and Park Valley, Utah (10 miles [16 km] to the west).

The Kelton Pass SE and Monument Peak SW 7.5′ quadrangles are located entirely within southern Curlew Valley, which drains south into Great Salt Lake, and extends north of the area shown on figure 1 into Idaho. Curlew Valley is bounded on the west by the Raft River Mountains and on the east by the Hansel Mountains (figure 1). Sedimentary and volcanic bedrock exposures within the quadrangles form the Wildcat Hills, Cedar Hill, and informally named Middle Shield (figure 1). Exposed rocks and deposits are Permian to Holocene in age, and include the Permian quartz sandstone and orthoquartzite of the Oquirrh Formation (Pos), tuffaceous sedimentary rocks of the Miocene Salt Lake Formation (Ts), Pliocene basaltic lava flows (Tb) and dacite (Tdw), Pleistocene rhyolite (Qrw) and basalt (Qb), and Pleistocene and Holocene surficial deposits of alluvial, lacustrine, and eolian origin. Structurally, the map area is situated in the northeastern Basin and Range Province, and is inferred to lie within the hanging wall of the late Miocene detachment faults exposed in the Raft River Mountains to the northwest (e.g., Wells, 1992, 2009; figure 1).

This mapping project was undertaken to produce a comprehensive, large-scale geologic map of the Wildcat Hills, as well as to improve understanding of the volcanic and tectonic evolution of southern Curlew Valley. The resultant publication includes a geologic map of the Kelton Pass SE and Monument Peak SW quadrangles (plate 1), two interpretive geologic cross sections (plate 2), new geophysical data and interpretations, and new geochronology data for volcanic units within and near the quadrangles.

METHODS

Geologic mapping for this project was conducted as part of an ongoing cooperative agreement between the U.S. Geological Survey (USGS) and Utah Geological Survey (UGS) to complete intermediate-scale maps of the Grouse Creek and Tremonton 30′ x 60′ quadrangles (Miller and others, 2012; Miller and others, in preparation; Miller and Felger, in preparation). Previous studies (described below) provided an indispensable starting point for understanding the geologic units, stratigraphic relations, and geologic history of the area. Prior to starting fieldwork, geologic maps and sample locations from previous investigations were digitally compiled to compare previous observations and interpretations. Geologic fieldwork was conducted during the summers of 2006–2008, and geophysical fieldwork took place during the summers of 2011–2013. The quadrangles, which include a mixture of U.S. Bureau of Land Management (BLM), state, and private land, were accessed via four-wheel-drive vehicle, and on foot. Observations, recorded at hundreds of locations within the map area, included a description of the physical characteristics and stratigraphic relationships of the geologic unit(s), attitude of bedding and/or flow-foliation/lineation, photographic documentation of the site, and sample collection. Observation locations and traverse lines were recorded with hand-held GPS, and subsequently downloaded into ArcGIS and used as a guide during map compilation. Black-and-white stereo aerial photographs flown by the Army Map Service in May and June 1953 (1:62,400 scale) and the USGS in July 1967 (1:24,000 and 1:32,000 scale), were used to help discern features and relationships not easily visible on the ground or on a topographic map and to map many of the surficial geologic units. Mapping was compiled in ArcGIS using 2006 National Agricultural Imagery Program (NAIP) color and color-infrared Digital Orthophoto Quadrangles (DOQs), black-and-white DOQs, 1:24,000-scale Digital

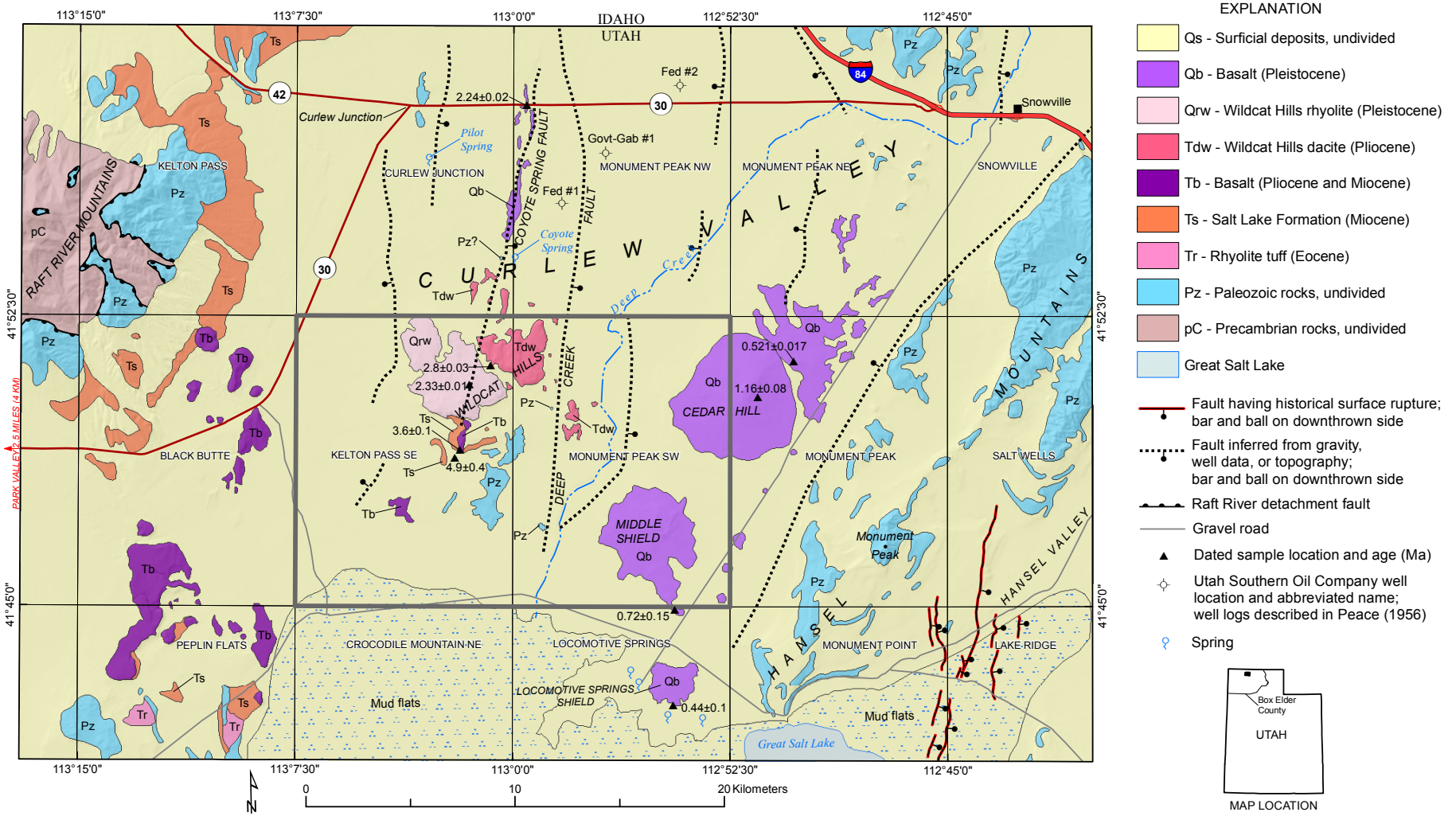

Figure 1. *Index map showing location of Kelton Pass SE and Monument Peak SW quadrangles (thick gray line), adjacent 7.5' quadrangles, primary geographic features, generalized geology, and locations of radiometric ages listed in table 1. Only new ages are shown for units Qrw and Tdw. Geology modified from Doelling (1980), Miller (1997a-c), Miller and Langrock (1997a-c), Wells (2009), authors' mapping, and U.S. Geological Survey (2015) fault database.*

Raster Graphics (DRGs), and 5- and 10-meter Digital Elevation Models (DEMs) as base materials.

Felger mapped the bedrock geology in the Kelton Pass SE quadrangle, refined the bedrock geology in the Monument Peak SW quadrangle (Miller and Langrock, 1997b), and digitally compiled the map and cross sections. Miller mapped the surficial geology in the Kelton Pass SE quadrangle, refined the surficial geology in the Monument Peak SW quadrangle, and performed U-Pb analysis of zircons. Langenheim compiled, collected, processed, and interpreted geophysical data and created geophysical models of cross sections. Fleck performed $^{40}Ar/^{39}Ar$ analysis of volcanic units at the USGS geochronology laboratory in Menlo Park, California.

PREVIOUS STUDIES

The *Geologic Map of Northwestern Utah* (Stokes, 1963) depicts the geology of the Kelton Pass SE and Monument Peak SW quadrangles as outcrops of late Tertiary rhyolite-dacite-quartz latite flows and pyroclastics, late Tertiary basalt and basaltic andesite flows, and Lower Permian and Pennsylvanian Oquirrh Formation, overlain by a mantle of Quaternary alluvial, colluvial, and lacustrine deposits. Subsequent mapping and topical studies included a geologic map and description of the geology of the Wildcat Hills (Howes, 1972), a regional-scale geologic map of Box Elder County, Utah (Doelling, 1980), a petrologic study of the volcanic rocks of the Wildcat Hills (Shea, 1985), a petrologic study of the Curlew Valley basalt flows (Kerr, 1987), a study of Pliocene and Quaternary volcanism in the northern Great Salt Lake area (Miller and others, 1995), and an interim geologic map of the Monument Peak SW quadrangle (Miller and Langrock, 1997b). Miller and others (1995) published seven K-Ar ages (table 1) for lava flows in the area of figure 1, establishing that some of the volcanic rocks in Curlew Valley range from Pliocene to Pleistocene in age.

Regional geophysical investigations (Cook and others, 1964; Zoback, 1983), and drill-hole logs from water wells (Baker, 1974; Utah Division of Water Rights, 2014) and oil exploration wells (Peace, 1956; Utah Division of Oil, Gas and Mining, 2012–2014) provide information about the subsurface geology of the Curlew Valley basin. A study of the geology and groundwater in Curlew Valley (Hurlow and Burk, 2008) synthesized new and existing surface, subsurface, and geophysical data to characterize the subsurface geology in the map area.

Studies of surficial deposits in southern Curlew Valley are mostly parts of regional investigations of Pleistocene lakes (Currey, 1982; Oviatt and Miller, 1997). Miller and others (1995, 2007) studied the basaltic Hansel Valley ash (estimated age ~26,500 ^{14}C yr B.P), which is an important stratigraphic marker bed found in Lake Bonneville deposits, and is thought to have erupted from an unidentified source in Curlew Valley. Photo-interpretation of surficial deposits of the Monument Peak SW quadrangle (Miller and Langrock, 1997b) provided a starting point for mapping the surficial deposits in the quadrangles.

GEOLOGIC OVERVIEW

Geology in the quadrangles consists of several hills underlain by late Cenozoic volcanic rocks, minor exposures of Tertiary basinal sedimentary rocks, and a few scattered outcrops of fractured Paleozoic rocks. Widespread mantles of alluvial, lacustrine, and eolian deposits cover much of the quadrangle, illustrating the history of Lake Bonneville and streams sourced from Curlew Valley and the Raft River Mountains (plate 1).

Volcanic rocks range from basalts (Qb) that form shield volcanoes in the east, a prominent plateau underlain by rhyolite lava (Qrw) that forms the western Wildcat Hills, and steep-sided thick flows or domes of dacite (Tdw) that form the eastern Wildcat Hills and isolated outcrops west of Deep Creek. Remnants of older basalt flows (Tb) occur in scattered outcrops south of the Wildcat Hills. Ages of the volcanic rocks, discussed below, indicate that the basalts in the shields are middle Pleistocene in age, the rhyolite and dacite are early Pleistocene to latest Pliocene, and the older basalt is early Pliocene. Details about vent location and eruptive history of these units are developed later in this report, along with interpretations of the subsurface geology derived from geophysical, geochronology, and mapping data.

GEOPHYSICAL DATA

Overview and Methods

Geophysical data in the quadrangles consist of gravity and airborne magnetic data that can help provide a subsurface framework for the surface geology. These data are sensitive to density and magnetization contrasts, physical properties that can serve as proxies for certain rock types. Gravity data are particularly well suited for determining the shape of Cenozoic basins because of the significant density contrast between dense pre-Cenozoic basement rocks and generally less dense Cenozoic rocks. Magnetic data reflect magnetization variations within the Earth's crust and are well suited for mapping the distribution of rock types that contain magnetite, such as mafic igneous rocks. Gravity and magnetic data can also be used to model the location and geometry of faults that juxtapose rocks and sediments of differing density and magnetic properties.

The gravity map (figure 2) was created from 138 measurements compiled from several sources. A majority of the measurements in Curlew Valley are from the study of Hurlow and

Table 1. *Summary of radiometric age analyses for volcanic units in or adjacent to Kelton Pass SE and Monument Peak SW quadrangles.*

Sample Number	Map Unit	Rock Name	7.5 ' Quadrangle	Latitude (N)	Longitude (W)	Age (Ma)	Material Dated	Lab	Method	Reference
M87LS-135	Qb	basalt	Locomotive Springs	41.707628	-112.908384	0.44 ± 0.1	whole rock	USGS	K-Ar	Miller and others (1995)
F06_437CV	Qb	basalt	Monument Peak	41.855807	-112.839310	0.521 ± 0.017	groundmass	USGS	$^{40}Ar/^{39}Ar$	this study
M89CV-44	Qb	basalt	Locomotive Springs	41.748818	-112.907742	0.72 ± 0.15	whole rock	USGS	K-Ar	Miller and others (1995)
M89CV-43	Qb	basalt	Monument Peak	41.840199	-112.859982	1.16 ± 0.08	whole rock	USGS	K-Ar	Miller and others (1995)
F06_098CV	Qb	basalt	Monument Peak NW	41.965880	-112.993291	2.238 ± 0.022	groundmass	USGS	$^{40}Ar/^{39}Ar$	this study
M93WI-40	Qrw	rhyolite	Kelton Pass SE	41.845317	-113.025920	2.1 ± 0.06	sanidine	USGS	K-Ar	Miller and others (1995)
F06_306CV	Qrw	rhyolite	Kelton Pass SE	41.845320	-113.026024	2.331 ± 0.010	sanidine	USGS	$^{40}Ar/^{39}Ar$	this study
F06_371CV	Tdw	dacite	Kelton Pass SE	41.853935	-113.013804	2.8 ± 0.03	zircon	USGS	U-Pb	this study
M93WI-37	Tdw	dacite	Kelton Pass SE	41.852431	-113.014387	4.4 ± 1.1	plagioclase	USGS	K-Ar	Miller and others (1995)
M93WI-43	Tb	basalt	Kelton Pass SE	41.817184	-113.031202	3.6 ± 0.1	whole rock	USGS	K-Ar	Miller and others (1995)
AD/WH/91-7	Tb	basalt	Kelton Pass SE	41.813861	-113.034297	4.9 ± 0.4	whole rock	Krueger	K-Ar	Miller and others (1995)

Notes:

Location data in NAD83.

Analytical data for new U-Pb and $^{40}Ar/^{39}Ar$ ages are shown in tables 2 and 3.

Whole rock samples are unseparated, crushed and sized multi-mineral aggregates of a rock. Groundmass samples are 'separates' derived by crushing a rock, then removing phenocrysts, magnetic minerals, and 'fines' and sorting the remaining material to produce a size fraction suitable for analysis.

Only new ages for units Qrw and Tdw (samples F06_306CV and F06_371CV) are shown on figure 1. Previous ages for these units (samples M93WI-40 and M93WI-37) are not shown on figure 1.

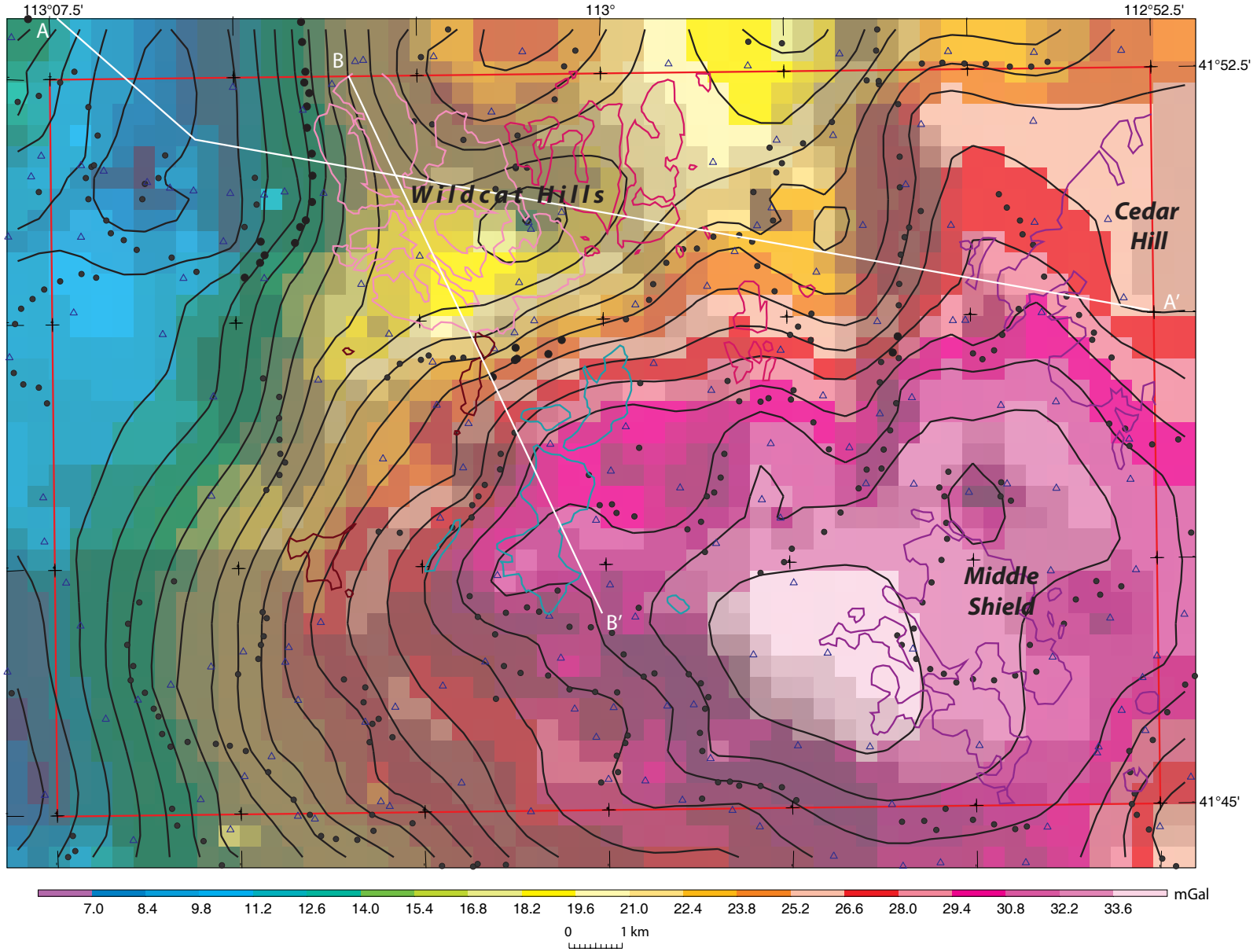

Figure 2. *Isostatic residual gravity map of the Kelton Pass SE and Monument Peak SW quadrangles (outlined in red). Data in mGal represented by color ramp and contour lines (black lines). Geologic cross section lines are shown in white; cross sections shown on plate 2. Blue triangles, gravity measurements. Small and large black dots, locations of maximum horizontal gradient less than and greater than mean value, respectively. Blue lines, outlines of Permian Oquirrh Formation outcrops; brown lines, Pliocene basalt; magenta lines, Pliocene dacite; pink lines, Pleistocene rhyolite; purple lines, Pleistocene basalt.*

Burk (2008), supplemented by data collected subsequently by the UGS and USGS (Langenheim and others, 2013, 2014). The data were processed using standard formulas to isostatic residual gravity values, which should reflect lateral density variations within the mid- to upper crust. This map removes the long-wavelength component of the gravity field assuming isostatic compensation, which provides a physics-based regional field. We further enhanced upper-crustal sources (figure 3) by upward continuing the field (i.e., mathematically filtering the data as if they had been measured at a higher elevation) by 3280 feet (1 km) and then subtracting the original field. This procedure emphasizes shorter-wavelength anomalies, which should be more closely related to the mapped geology.

The magnetic map (figure 4) is based on a fixed-wing aeromagnetic survey flown in July 2010 by Firefly Aviation Ltd for USGS and UGS. Data were collected at a nominal height of 1000 feet (305 m) above ground along east-west flight lines spaced 0.5 miles (800 m) apart. The average height of the aircraft above terrain in the map area was 1245 feet (380 m) and in the northwest corner of the study area the aircraft was as much as 2460 feet (750 m) above Utah Highway 30. North-south tie lines were flown 5 miles (8 km) apart. Data were adjusted for tail-sensor lag and diurnal field variations. Further processing included microleveling using the tie lines and subtraction of the reference field defined by International Geomagnetic Reference Field 2005 extrapolated to the time and elevation of data acquisition. Accuracy of this survey is 1 nanotesla (nT) or better. The survey is a considerable improvement on pre-existing data, which consisted of profiles flown 3 miles (4800 m) apart at a height of only 400 feet (120) m above ground as part of the National Uranium Resource Evaluation (NURE; Geodata International, Inc., 1979). The new survey particularly highlights short-wavelength magnetic anomalies associated with Cenozoic volcanic rocks.

To help delineate structural trends and gradients expressed in the gravity and magnetic fields, a computer algorithm was used to locate maximum horizontal gradients (Cordell and Grauch, 1985; Blakely and Simpson, 1986), which were then used to map concealed basin faults beneath the valley areas. We calculated magnetization boundaries on a filtered version of the magnetic field to isolate anomalies caused by shallow (<~3280 feet [1 km]) sources (figure 5), similar to that described for the filtered gravity field above, but by subtracting a magnetic field that was upward continued 330 feet (100 m) from the original magnetic field. Then the resulting residual aeromagnetic field was mathematically transformed into magnetic potential anomalies (Baranov, 1957); this procedure effectively converts the magnetic field to the equivalent "gravity" field that would be produced if all magnetic material were replaced by proportionately dense material. The horizontal gradient of the magnetic potential field was then calculated. Gradient maxima occur approximately over steeply dipping contacts that separate rocks of contrasting densities or magnetizations. For moderate to steep dips (45˚ to vertical), the error in the location of the physical property contrast is less than or equal to the depth to the top of that contrast (Grauch and Cordell, 1987).

Results

The gravity field in the quadrangles is dominated by a large gravity high that extends from the eastern part of the map area, across Cedar Hill, Middle Shield, and outcrops of Oquirrh Formation (Pos) (figures 2, 3, and 6). The apex of the high is offset about 1.2 miles (2 km) west of the top of Middle Shield volcano, suggesting that the source of the high does not arise solely from high-density basalt exposed at the surface. The high is part of a larger feature that extends beyond the map area, forming a northeast-trending, roughly rectangular area of elevated gravity values (figure 6). The northwest margin of the high passes south of the Wildcat Hills, which are underlain by a northeast-trending gravity low. North of the Wildcat Hills are two somewhat less prominent gravity highs that are aligned in a north-northwest direction extending to the Idaho-Utah border. The highest values in these highs correspond to small outcrops of Paleozoic sedimentary rocks exposed west of Coyote Spring and north of Pilot Spring at Curlew Junction (figures 1 and 6).

The western margin of the main gravity high has a northerly trend that appears to step eastward to the north towards and west of the Wildcat Hills, forming the eastern margin of a gravity low that lies between the Wildcat Hills and the Raft River Mountains (figure 6). The density boundaries that mark the eastern margin of the low likely reflect probable faults that bound a significant basin in the hanging wall of the Raft River detachment (northwest part of plate 1). This interpretation differs from that of previous workers (Cook and others, 1964; Hurlow and Burk, 2008), who suggested that the basin margin formed in a crustal downwarp between the Raft River Mountains and Wildcat Hills without significant influence from basin-bounding faults. Cook and others (1964) speculated that the downwarp was associated with crustal loading from thrust faults. We interpret this boundary as a fault because the additional gravity data show that the gradient is more prominent and linear; furthermore, west of the Wildcat Hills, the gradient coincides with a subtle magnetization boundary that can be reasonably interpreted as a structure that also down-dropped Neogene volcanic rocks. Another possible north-striking fault in the hanging wall of the detachment lies between Cedar Hill and the easternmost exposures of the dacite of Wildcat Hills (Tdw), nicely highlighted in the filtered gravity map (unnamed fault east of Deep Creek on plate 1; figure 3). The amplitude of the gravity gradient diminishes to the south, the gradient curving to the southwest as it approaches Middle Shield.

The magnetic map (figure 4) highlights the short-wavelength, high-amplitude anomalies associated with exposed Cenozoic volcanic rocks, forming strong magnetization boundaries that enclose the Quaternary basalts at Cedar Hill and Middle Shield and the more silicic volcanic rocks exposed in the Wildcat

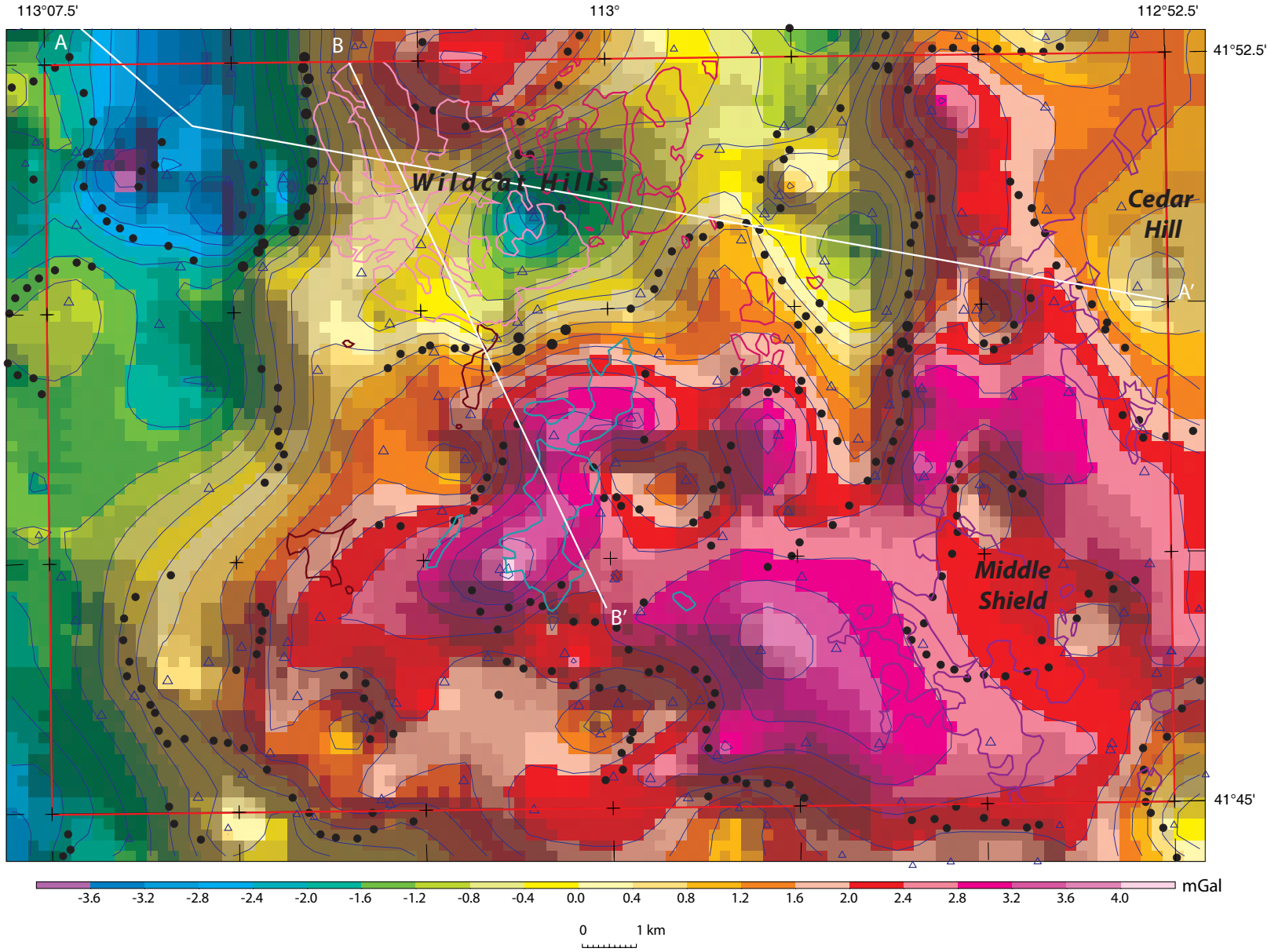

Figure 3. *Isostatic residual gravity map of the Kelton Pass SE and Monument Peak SW quadrangles (outlined in red) filtered to enhance shallow depth sources (< 6 miles [10 km]). Geologic cross section lines are shown in white; cross sections shown on plate 2. Blue triangles, gravity measurements. Small and large black dots, locations of maximum horizontal gradient less than and greater than mean value, respectively. Blue lines, outlines of Permian Oquirrh Formation outcrops; brown lines, Pliocene basalt; magenta lines, Pliocene dacite; pink lines, Pleistocene rhyolite; purple lines, Pleistocene basalt.*

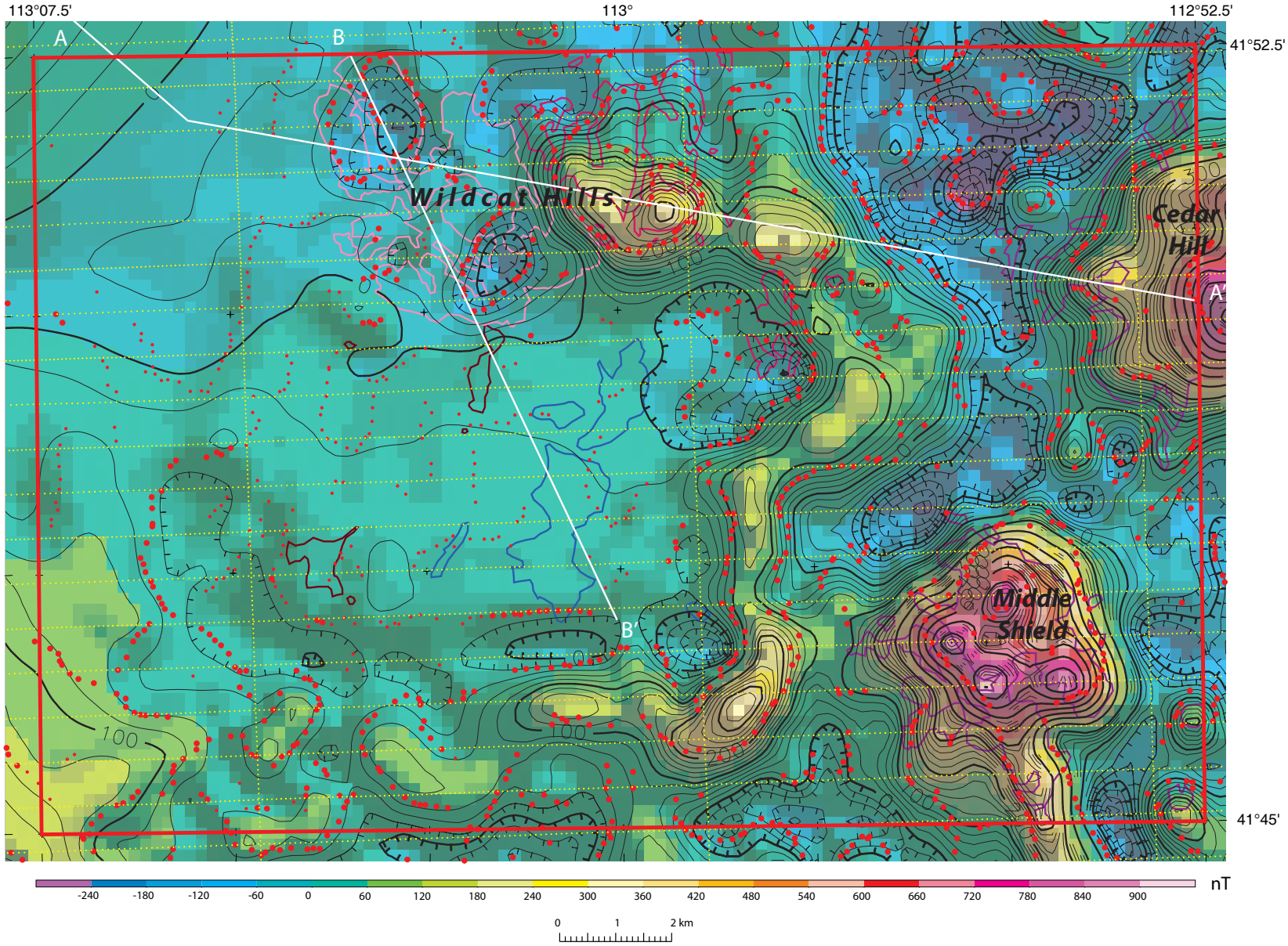

Figure 4. *Aeromagnetic map of the Kelton Pass SE and Monument Peak SW quadrangles (outlined in red). Geologic cross section lines are shown in white; cross sections shown on plate 2. Data in nT represented by color ramp and contour lines (black lines). Yellow dotted lines, flight tracks. Small and large red dots, locations of maximum horizontal gradient less than and greater than mean value, respectively. Blue lines, outlines of Permian Oquirrh Formation outcrops; brown lines, Pliocene basalt; magenta lines, Pliocene dacite; pink lines, Pleistocene rhyolite; purple lines, Pleistocene basalt.*

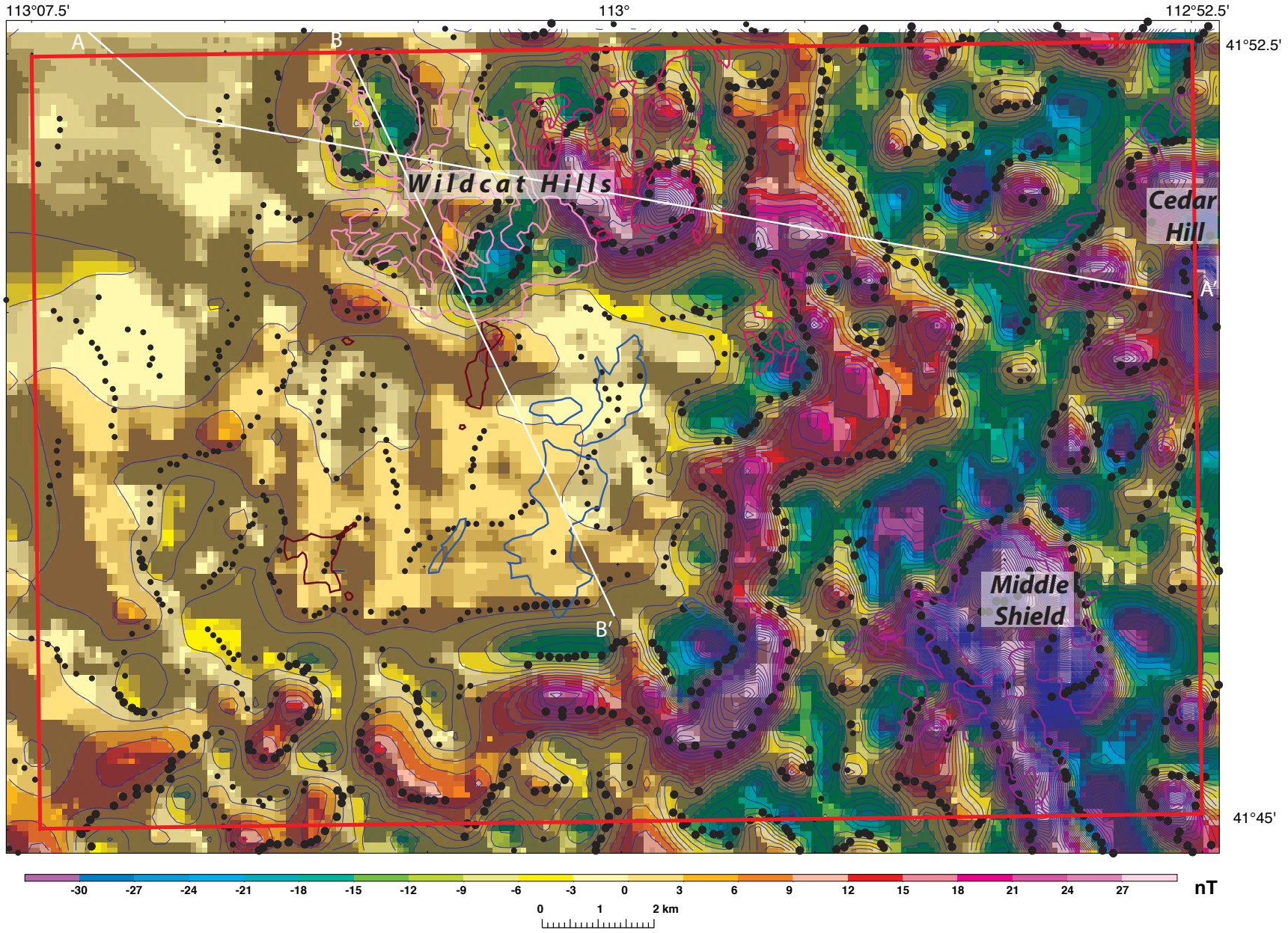

Figure 5. *Aeromagnetic map of the Kelton Pass SE and Monument Peak SW quadrangles (outlined in red) filtered to enhance shallow depth sources (< 3280 feet [1 km]). Geologic cross section lines are shown in white; cross sections shown on plate 2. Small and large black dots, locations of maximum horizontal gradient less than and greater than mean value, respectively. Blue lines, outlines of Permian Oquirrh Formation outcrops; brown lines, Pliocene basalt; magenta lines, Pliocene dacite; pink lines, Pleistocene rhyolite; purple lines, Pleistocene basalt.*

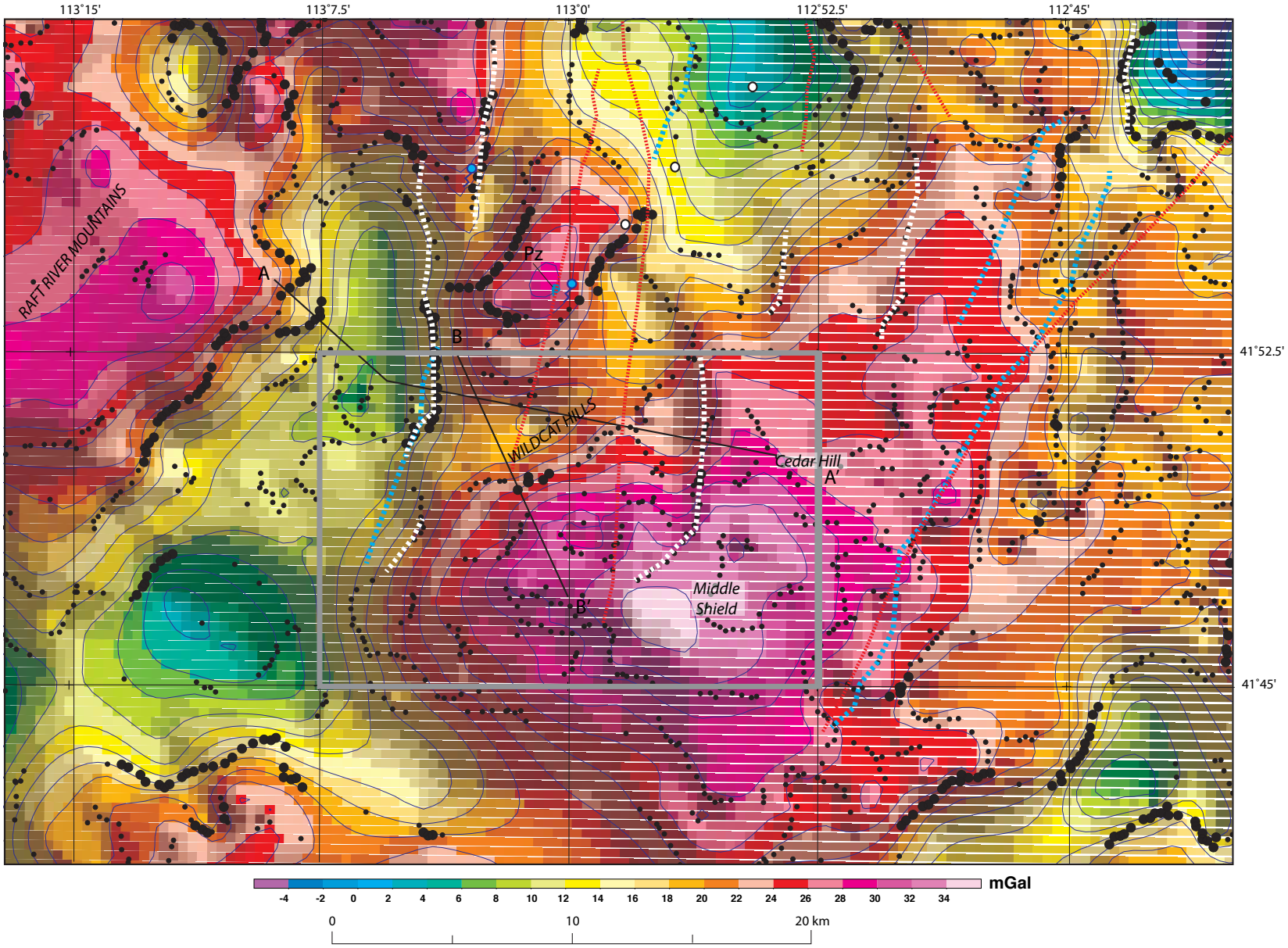

Figure 6. *Isostatic residual gravity map of the index area shown on figure 1. Kelton Pass SE and Monument Peak SW quadrangles outlined in gray. Geologic cross section lines are shown in medium-weight black; cross sections shown on plate 2. Small and large black dots, locations of maximum horizontal gradient less than and greater than mean value, respectively. White dashed lines, faults inferred from gravity data; blue dashed lines, faults inferred from aeromagnetic data, and red dotted lines, additional faults from figure 1. White circles, oil exploration wells; blue circles, springs (see figure 1). Pz, location of Paleozoic bedrock outcrop.*

Hills. Similar strong magnetization boundaries extend beyond the exposures of these rocks (figure 7). The anomalies delineated by these magnetization boundaries wrap around to the north, east, and south of the exposures of Oquirrh Formation (Pos) in the central part of the map (figures 4 and 5) and contrast with the relatively smooth magnetic pattern associated with the Oquirrh Formation. Within this smooth pattern are outcrops of Tertiary basalt that correspond to subtle anomalies that are enhanced in the filtered magnetic map (figure 5). These anomalies share many of the characteristics of the anomalies in the eastern part of the map, but the amplitudes of the anomalies are considerably diminished. The weak expression of these exposed basalts suggests that they are either very thin or consist of a stack of thin flows with normal and reversed magnetizations that essentially nearly cancel out. We prefer the first explanation since flows exposed in the map area and adjacent Black Butte and Peplin Flats quadrangles (figure 1) are thin and spatially limited in extent. In general, the western part of the map has more subdued magnetic expression of the volcanic rocks, likely because they are more deeply buried in basins outlined by the gravity low.

DRILL HOLE DATA

Logs for water wells (Baker, 1974; Hurlow and Burk, 2008; Utah Division of Water Rights, 2014) and oil exploration drill holes (Peace, 1956; Utah Division of Oil, Gas and Mining, 2012–2014) were a source of subsurface information, but limited by geographic distribution, depth extent, and log quality. Approximately 30 water wells have been drilled in low-lying parts of the map area for agricultural purposes. They range in depth from 64 to 510 feet (20 to 155 m), with most about 200 feet (60 m) deep. The logs are of varying quality; most, however, describe deposits of unconsolidated, poorly sorted, clay to boulder size sediments that are consistent with Quaternary alluvial deposits, and in some cases, possibly Pliocene deposits that post-date the Salt Lake Formation (Ts). In the vicinity of the Quaternary shield volcanoes, basalt was typically encountered within tens of feet (m) below the surface. Wells (B-13-10)11dcd-1 and (B-13-10)34ddc-1 (plate 1) are both about 2 miles (3.2 km) west of the westernmost outcrops of Quaternary basalt, and the logs (Baker, 1974) record basalt at depths less than 70 feet (20 m). A well located about 1 mile (1.6 km) west of the Wildcat Hills (plate 1, 27957) has a log (http://waterrights.utah.gov/cgi-bin/docview.exe?Folder=welllog27957) that describes layers of "black limestone" from 60 to 280 feet (18 to 85 m), and "black limestone" with some broken areas from 280 feet (85 m) to the bottom of the hole at 340 feet (100 m). The "black limestone" is puzzling, and we speculate that it was misidentified and is actually basalt. The basalt flows in this area are typically thin, fine-grained, phenocryst-poor, and have calcite alteration, making misidentification as limestone a reasonable possibility, especially in cuttings. This interpretation is supported by the magnetic data (figure 5) which shows a subdued positive anomaly in the area of the well that is similar to the signature associated with nearby basalt outcrops. The depth to bedrock predicted by analysis of the gravity data at the well location is about 1650 feet (500 m), which is significantly deeper than the bottom of the well, also suggesting that it might be basalt.

No wells have been drilled into the volcanic units of the Wildcat Hills. Hurlow and Burk (2008) show a well was drilled to a depth of 179 feet (55 m) in the middle of the Wildcat Hills rhyolite (Qrw) (their figure 21, ID 37), and they depict the lithologic information from the driller's log on their cross section E-E′. We found this well was mislocated in the Hurlow and Burk (2008) report. The drill hole is actually located in the SW1/4 section 18, T. 13 N., R. 11 W, which is about 6 miles (10 km) west in the Black Butte quadrangle (figure 1).

An oil exploration drill hole (plate 1, SP) was drilled by the Stanford Petroleum Company in 1946 to a depth of 679 feet (207 m) just south of the Wildcat Hills, in section 25, T. 13 N., R. 11 W. Despite ambiguities concerning the location (J. King, UGS, written communication, January 2012), and the near illegibility of the log (http://oilgas.ogm.utah.gov/wellfiles/003/4300320083.pdf), it seems to indicate that Pennsylvanian-age rocks (inferred to be Oquirrh Formation) were encountered at the surface. No outcrops of Paleozoic rocks are present at that location, but it is reasonable that Oquirrh Formation (Pos) is present at a relatively shallow depth in the subsurface. The relatively smooth pattern in the magnetic data (figure 4) is consistent with this interpretation.

STRUCTURAL GEOLOGY

Curlew Valley is a complex valley that is wider than most in northern Utah. Structurally, it lies in the hanging wall of the late-middle Miocene Raft River detachment fault (e.g., Wells, 1992, 2009), and consists of a pair of north-trending basins and an intervening bedrock ridge that may be a horst. Structures within the quadrangles are difficult to map because of widespread mantling by Lake Bonneville deposits and low relief, as well as being obscured by Pliocene and Pleistocene lava flows. Although evidence for Cenozoic structure within the quadrangles is not striking, geophysical data and mapping in adjacent quadrangles help to inform interpretation of subtle features in the map area.

Oquirrh Formation (Pos) outcrops of quartz sandstone and orthoquartzite south of the Wildcat Hills (plate 1) are highly fractured, possibly due to deformation that occurred within the hanging wall of the Raft River detachment fault. Measured planar features may mark bedding plane partings or may be tectonic in origin. The massive, well-sorted nature of the formation, combined with subsequent brecciation, precludes confidently identifying the origin of the features, and thus they are labeled as "planar features of uncertain origin" (plate 1).

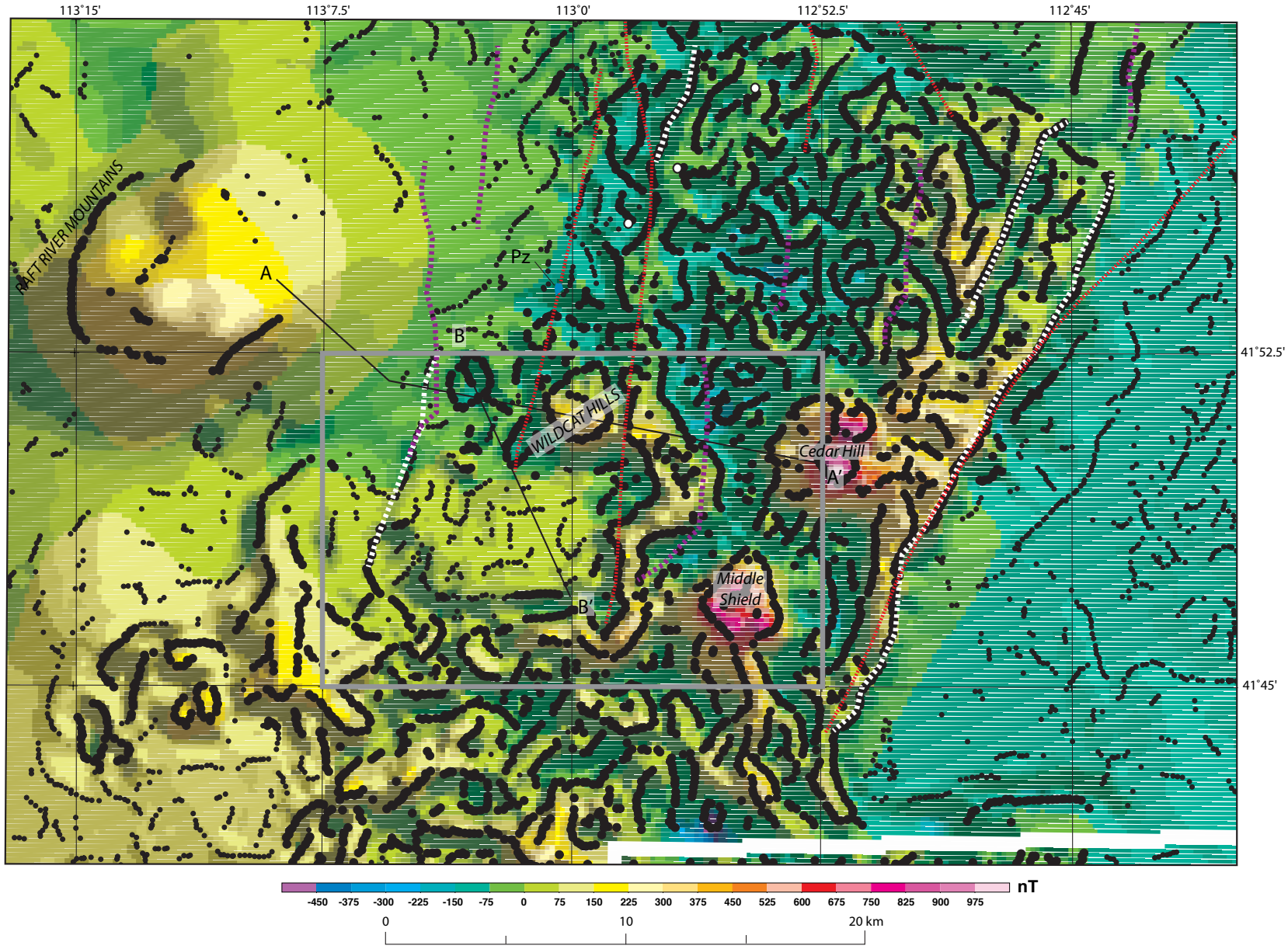

Figure 7. *Aeromagnetic map of the index area shown on figure 1. Kelton Pass SE and Monument Peak SW quadrangles outlined in gray. Geologic cross section lines are shown in medium-weight black; cross sections shown on plate 2. Small and large black dots, locations of maximum horizontal gradient less than and greater than mean value, respectively. White dashed lines, faults inferred from aeromagnetic data; purple dashed lines, faults inferred from gravity data, and red dotted lines, additional faults from figure 1. White circles, oil exploration wells (see figure 1). Pz, location of Palezoic bedrock outcrop.*

Complexly folded and tilted tuffaceous sedimentary rocks of the Salt Lake Formation (Ts) overlie the brecciated rocks of the Oquirrh Formation (Pos). The contact between the two units is not exposed; however it is inferred to be an erosional unconformity, based on the presence of thin, discontinuous deposits of reddish, calcareous clay with pebbles and cobbles of calcareous quartz sandstone, and less abundant limestone and dark chert that occur locally on the Oquirrh Formation (Pos). The deposits (Paleosol location, plate 1) are inferred to be remnants of a paleosurface or pediment developed on the Oquirrh Formation (Pos) prior to deposition of the Salt Lake Formation (Ts). Similar deposits have been observed at the unconformity between the Oquirrh Formation and Salt Lake Formation in the North Promontory Mountains to the east (Miller and Felger, in preparation). John and others (2012) document a somewhat similar scenario in the Bodie Hills volcanic field, California and Nevada, where the Miocene volcanic rocks were erupted onto an erosional surface of pre-Tertiary basement rocks that is marked locally by remnants of a paleosol. The physical characteristics of the inferred paleosol deposits in the map area are similar to those observed in the Bodie Hills (D. John, USGS, written communication, March 17, 2015). Alternatively, the deposits may represent eroded remnants of Permian or Triassic strata, early-stage basin-fill deposits such as the Paleocene to Eocene-age Wasatch Formation, or a facies of the Salt Lake Formation (Ts), such as the red conglomerate of Todd (1983).

Bedding attitudes in Salt Lake Formation (Ts) strata south of the Wildcat Hills are variable over short vertical and lateral distances (plate 1), making it difficult to characterize the geometry of the unit in a meaningful way. Near-vertical beds exposed in section 25 define a small, steeply southwest-plunging synform, and outcrops east and west of the main exposure of Tertiary basaltic lava flows (Tb) appear to form a northeast-trending, gently plunging syncline (plate 1; plate 2, B-B′). The folds are similar to those observed on the east flank of the Raft River Mountains, where Wells (2009) observed that Tertiary strata are involved in long-wavelength folds that plunge southwest and are related to either D_6 or D_7 deformational events (middle to early late Miocene). The complex nature of the bedding in the study area may indicate that the Salt Lake Formation (Ts) overlies the Oquirrh Formation (Pos) on a low-angle fault, as opposed to an erosional unconformity. This interpretation would be consistent with observations in the Kelton Pass quadrangle to the west, where Wells (2009) noted that Tertiary sedimentary rocks had variable bedding attitudes suggestive of folding and tilting, and that the contact between Paleozoic and Tertiary rocks was typically a fault.

Very little direct evidence for faulting was observed within the quadrangles. A few small, discontinuous fault planes and fractures (none mapped) are present in outcrops of the Salt Lake and Oquirrh Formations. They are near-vertical, with strikes between north and N. 45º E., and variable directions of dip. Sense of motion, where determinable from striae or offset beds, is typically dip-slip, although one outcrop has striae indicating strike-slip motion. Where amount of offset could be determined, it was limited to less than a few feet (< 1 m). None of these structures appear to be parts of major fault zones because they are isolated and discontinuous.

Indirect evidence for the presence of faults, however, is abundant, and includes vegetation lineaments in Quaternary surficial deposits (plate 1), topographic scarps and ”grooves” in the rhyolite (Qrw) and dacite (Tdw), alignment of the vents that produced several of the Quaternary and Pliocene lava flows (plate 1, figure 1), and geophysical data discussed previously. The vegetation lineaments, which are readily visible as dark lines on aerial imagery, are prevalent on both sides of Deep Creek (plate 1). They are mapped conservatively where parallel to straight segments of drainages and lake shore features with which they might be confused. The lineaments are not generally noticeable on the ground; however, we observed the vegetation associated with some lineaments to be substantially thicker and/or taller than in adjacent areas, suggesting a connection with the groundwater system in some cases. These lineaments and the topographic alignments typically trend north to northeast, parallel to the general trend of Curlew Valley and the prominent fault along its east margin (figure 1). In addition to the inferred faults described in the geophysical data section, two other concealed faults are inferred—the Deep Creek and Coyote Spring faults (figure 1, plate 1).

The Deep Creek fault lies between the Wildcat Hills and Deep Creek, and strikes approximately N. 10º E. (plate 1). At its southern end it is drawn in the covered area between an outcrop of Oquirrh Formation (Pos) and outcrops of Quaternary basalt (Qb) that form Middle Shield that are at approximately the same elevation. Subtle gradients in the magnetic and gravity data may represent continuation of the fault to the south (figures 6 and 7). Farther north it is drawn in the covered area between a small outcrop of Oquirrh Formation (Pos) and outcrops of dacite (Tdw) to the east that are at equivalent and lower elevations. This relation may reflect fault throw, with displacement down to the east. Alternatively, it may represent paleotopography, with the dacite (Tdw) erupting onto a surface that was at a lower elevation than the Oquirrh Formation (Pos) outcrop to the west. Where the fault intersects cross section line A-A′, a saddle in the aeromagnetic high associated with the dacite (Tdw) outcrops in the eastern Wildcat Hills (figures 4 and 5) might be an expression of the fault. The fault is inferred to continue north-northeastward between the Federal No.1 and Government-Gabrielson No. 1 exploration wells (figure 1). Logs for those wells (Peace, 1956) show that basalt flows in the Government-Gabrielson No. 1 well were penetrated 130 to 325 feet (40 to 100 m) lower than possibly equivalent flows in the Federal No. 1 well to the west. Similarly, the contact between Oquirrh Formation and Tertiary or pre-Tertiary rocks was penetrated 3460 feet (about 1 km) lower in the Government-Gabrielson No. 1 well than in the Federal No. 1 well. This offset is consistent with a down-to-the-east normal fault, or could be reflecting paleotopography.

The Coyote Spring fault extends from just south of the Wildcat Hills to just north of Utah State Highway 30 (plate 1, figure 1). It strikes approximately N. 15º E. and is best expressed as a series of low, discontinuous, east-facing scarps in Quaternary basalt flows (Qb) north of the quadrangles. The scarps begin north of the map area, about 1 mile (1.6 km) southwest of Coyote Spring, and extend north-northeast to just north of Utah State Highway 30 (figure 1). It is unclear if the flows are actually offset across the scarp; however, the flows on the east lie 20 to 50 feet (5 to 15 m) lower than those on the west, consistent with offset across a down-to-the east normal fault. Similarly, Oquirrh Formation outcrops appear to be offset across the scarp. A small outcrop (Pz on figure 1) is exposed at an elevation of about 4470 feet (1360 m) on the west side of the scarp about 0.5 mile (1 km) west of Coyote Spring (figure 1). On the east side of the scarp in the Federal No. 1 well (figure 1), rocks assigned to the Oquirrh Formation are recorded at 3980 feet (1213 m) (Peace, 1956), suggesting offset across a fault of up to 500 feet (150 m) (plate 2, A-A′ and B-B′). The fault has no obvious expression in the gravity data and is oriented obliquely to the main gravity gradient, which trends more to the northeast (figure 6). However, the drop in gravity values between the outcrop of Oquirrh Formation (Pos) and the drill hole is consistent with Oquirrh strata being lower in the drill hole, and the fault does coincide with a subtle boundary in the aeromagnetic data (figure 7). Hurlow and Burk (2008) also characterize the scarp as representative of an east-side-down normal fault.

The Coyote Spring fault apparently controls groundwater discharge, as indicated by seeps and springs that are present along the southern end of the scarp. Coyote Spring (figure 1) is especially interesting because it has a temperature of 43.5ºC (110ºF), which is about 30ºC warmer than other springs measured in Curlew Valley (Hurlow and Burk, 2008), and requires much deeper sources of water. The presence of warm springs suggests that the fault is a major crustal feature that disrupts deep groundwater flow paths. Similarly, the fault appears to have influenced the location of the eruptions that produced the Quaternary basalt (Qb), which is 2.2 Ma, and the Wildcat Hills rhyolite (Qrw), which is 2.3 Ma (figure 1, table 1). The Quaternary basalt flows (Qb) are tightly distributed along the fault, and the three highest peaks of the Wildcat Hills (plate 1) overlie one of the vent areas for the rhyolite (Qrw) in a north-northeast alignment that is on trend with the fault (figure 1). An abrupt lithologic change occurs across a gully in Salt Lake Formation (Ts) strata underlying the rhyolite (Qrw) and basalt (Tb) south of the Wildcat Hills. The gully is approximately on trend with the peaks, and is inferred to be a poorly-exposed portion of the fault.

The Coyote Spring fault has no definitive expression in the gravity or magnetic data in the quadrangles. As was the case to the north, the fault is oriented obliquely to the main gravity gradient, which trends more to the northeast (figure 6). A northeast-trending gravity low underlies the Wildcat Hills rhyolite (Qrw) and dacite (Tdw), with the deepest part of the low occurring on the east side of the inferred Coyote Spring fault (figures 2, 3, and 6). This drop in the gravity field from west to east can be explained by the presence of a thicker section of Salt Lake Formation (Ts) on the downthrown side of a down-to-the east normal fault (plate 2, A-A′).

GEOLOGIC CROSS SECTIONS

The first published geologic cross sections of southern Curlew Valley were developed by Hurlow and Burk (2008) as part of their study of the greater Curlew Valley groundwater system. They used existing and newly-collected gravity data in conjunction with available aeromagnetic data to help delineate the subsurface structure of the Curlew Valley depositional basin. Part of this process involved constructing geologic cross sections that subsequently were used to generate predictive models of the gravity and magnetic data along the line of section. The predictive models were compared to the observed gravity and magnetic data, and the cross sections modified as necessary to produce a better fit to the observed data. Cross sections E-E′ and F-F′ of Hurlow and Burk (2008), and the geophysical models shown on their figures 18 and 19 partially intersect the quadrangles and provided a useful frame of reference during the development of our cross sections.

Development of our cross sections followed a process similar to that of Hurlow and Burk (2008). Topographic profiles, segmented by geologic unit, were generated in ArcGIS for each section line, using the 10-meter DEM and geologic unit polygons as input. The subsurface geometries of geologic units and structures were digitized using assumptions about existence, thickness, and orientation that were derived from field observations, well log information, and geophysical data. The cross sections were imported into geophysical modeling software (GM-SYS), and the geologic unit polygons were assigned density and magnetization values based on field measurements for the units. Gravity and magnetic anomalies were calculated for the assigned density and magnetization contrasts in the cross sections and then compared to the observed values for the same lines of section. Based on the comparison, the thickness and geometry of units in the original cross sections were adjusted as needed in an attempt to meet the constraints of both the geologic and geophysical data.

Hurlow and Burk (2008) made the important statement that geophysical models are non-unique, and other workers could derive different cross sections from the same data, especially if more refined estimates of the density and magnetic susceptibility are used for the geologic units. We improved the models with refined density and magnetic susceptibility values based on rock measurements from the area, and also included remanent magnetization for those units that produced negative anomalies. We also incorporated considerably higher-resolution aeromagnetic data collected in 2010, and additional gravity measurements that were made specifically to improve the characterization of units and structures in the map area.

The improved data, in conjunction with a study area that was considerably smaller than that of Hurlow and Burk (2008), allowed us to conduct detailed analysis and integration of the geophysical data and surface geology for the map area. As a result, our section A-A′, which is roughly parallel to part of their E-E′ and a geophysical model shown on their figure 18, is considerably different than theirs.

Previous workers described the subsurface geology between the Wildcat Hills and Curlew Junction (figure 1) as a shallowly-buried, north-northwest-trending bedrock ridge or structural high of Paleozoic rocks that separates the structural basins that underlie Curlew Valley (Baker, 1974; Miller and Langrock, 1997b; Hurlow and Burk, 2008). Exposures of Oquirrh Formation (Pz) south of the Wildcat Hills, west of Coyote Spring, and at Curlew Junction (figure 1) represent the barely-exposed top of the ridge. The gravity field is generally higher across this area (figure 6), and the western margin is well-delineated by the unnamed fault highlighted by a gravity gradient that lies just west of the Wildcat Hills. However, the gravity data also reveal the presence of northeast-trending gravity lows under the Wildcat Hills and southeast of Pilot Spring (figures 1 and 6), indicating that the bedrock ridge is more complicated than a simple fault-bounded tilt-block or horst. Interestingly, the trend of the anomalies over the bedrock ridge is similar to some of the fold axes attributed to the open folding (D_5) deformation event that produced broad, upright folds in rocks of the lower and middle allochthons in the Raft River Mountains (Wells, 2009). Perhaps this pattern reflects structures that formed during evolution of the Raft River Mountains metamorphic core complex, whereas more northerly-trending structures may be the result of more recent Basin and Range extension (Felger and others, 2011).

We considered several possible scenarios to explain the approximately 8 to 12 mGal gravity low that underlies the rhyolite (Qrw) and dacite (Tdw) of the Wildcat Hills. The simplest explanation is a thick section of Salt Lake Formation (Ts) that underlies the lava flows. Modeling of the geophysical data along cross sections A-A′ and B-B′ (plate 2) determined as much as 2500 feet (760 m) of low-density material consistent with Salt Lake Formation (Ts) could be present under the Wildcat Hills and fully account for the gravity low. However, this thickness seemed excessive in the context of the surface geology, so other explanations were explored. The co-location of the gravity low with the relatively low-density rhyolite (Qrw) and dacite (Tdw) flows suggested that felsic intrusions related to those units could be present in the basement. Geophysical modeling of that scenario along cross section line B-B′ determined that a body with the density of quartz (2620 kg/m^3) would need to be about 6 miles (10 km) in diameter, and extend from the near-surface to a depth of 13 miles (21 km) to produce the low. Such a large body to account for the extrusives at the surface also seems excessive. Another complicating factor is the big northeast-trending gravity high that extends westward from Cedar Hill and Middle Shield under the outcrops of Oquirrh Formation (Pos) (figure 2). This anomaly cannot be explained entirely by the Quaternary basalt shields and associated flows (Qb), and must be reflecting the presence of additional mafic material, such as a sill complex, at depth in the basement (Langenheim and others, 2011). Adding a mafic body that is about 6500 feet (2 km) thick at a depth of about 2 miles (3 km) can also fit the gradient that bounds the southern margin of the low along cross section line B-B′. Based on these scenarios and the constraints of the surface geology, we depict the subsurface geology of the Wildcat Hills as a half-graben with a moderate thickness of Salt Lake Formation (Ts) (plate 2, A-A′ and B-B′). The half-graben geometry is similar to that shown by Covington (1983) for the eastern Raft River Basin to the north.

The unnamed fault inferred from gravity data that lies between Cedar Hill and the easternmost exposures of the dacite of Wildcat Hills (Tdw) (plate 1) also was problematic to reconcile with the exposed geology. It is based on a north-south trending gravity gradient that indicates lower density material is present on the west side of the gradient (figures 2, 3 and 6). This geometry can be interpreted as a down-to-the-west normal fault with low-density basin fill such as the Salt Lake Formation (Ts) occupying the low on the west side of the fault and Paleozoic basement and basalt flows occupying the high on the east side of the fault. Thus, the gravity low on the west side of the fault is the southern part of a deep Cenozoic basin to the north (figure 6) that has about 3000 feet (1 km) of Tertiary sedimentary rocks, with interbedded basalt flows in the upper 600 feet (180 m) (Peace, 1956). According to this interpretation, the covered area between the Deep Creek fault and the unnamed fault on cross section A-A′ could be a shallow graben with dacite (Tdw) and possibly Tertiary basalt flows (Tb) overlying Salt Lake Formation (Ts), in turn overlying Oquirrh Formation (Pos). However, the exposures closest to the unnamed fault in the map area are the dacite (Tdw) west of the fault and Quaternary basalt (Qb) on the east side, indicating the opposite sense of offset. In this scenario, the gravity gradient would be accounted for by low-density dacite (Tdw) on the west juxtaposed against thick Quaternary basalt flows (Qb) on the east. The absence of a significant magnetic gradient does not support this scenario and the gravity high does not extend over Cedar Hill, as would be expected if Quaternary basalt flows were the primary cause of the gravity high. However, because of the ambiguities of interpreting the geophysical data, we depict the fault as down-to-the-east to adhere to the constraints of the exposed units (plate 1; plate 2, A-A′).

NEW GEOCHRONOLOGY DATA

New ages for the Wildcat Hills dacite (Tdw), rhyolite (Qrw), and previously undated basalt flows north of the Wildcat Hills and northeast of Cedar Hill (figure 1) were obtained as part of this project, and are summarized in table 1. These new data helped improve our understanding of the eruptive history of the Wildcat Hills and southern Curlew Valley.

Zircon U-Pb Data

The dacite (Tdw) had a poorly-constrained K-Ar plagioclase age of 4.4 ± 1.1 Ma (Miller and others, 1995) (sample M93WI-37, table 1, plate 1), and was a top priority for reanalysis. Plagioclase is present as both phenocrysts and xenocrysts, suggesting a mixed magma origin that is difficult to identify with $^{40}Ar/^{39}Ar$ analysis. We opted to date individual zircon grains by U-Pb to evaluate the presence of several ages of zircon growth. Sample F06_371CV (table 1, plate 1) was collected about 600 feet (180 m) north-northeast of sample M93WI-37. The zircon grains were imaged by cathode luminescence, which revealed that many are resorbed (figure 8) and are anhedral to subhedral. Some are broken, and all are relatively small with typical long diameters of 100 to 200 microns. All exhibit oscillatory zoning, but the grains range considerably from U-rich to U-poor. Some grains contain two parts, an inner (core) of sometimes poorly zoned zircon discordantly surrounded by the outer part of sharply zoned zircon.

We analyzed 27 zircon grains, eight of which were analyzed in two places, which resulted in 35 total analyses (table 2). The eight core-rim pairs were targeted to address possible discordance between core and outer parts, and to address the time involved in growth. We avoided metamict zircon cores, which may have been relic Precambrian grains, and parts of grains with many melt inclusions. Typical grains, and locations of the regions analyzed in each, are shown on figure 8. Results range from 2.6 to 4.3 Ma with most in the 2.7 to 3.1 Ma range (table 2). Four analyses revealed high common Pb (>6%), and others were slightly to moderately discordant. Because zircon is very retentive, old zircons from earlier parts of the magma evolution or even from digested rocks are possible. The data can be analyzed many ways. A culled data set that features only concordant analyses with low common Pb, U, and Th/U yields a coherent group of 19, whose weighted mean age is 2.80 ± 0.03 Ma (figure 9). Another approach is to select distinct populations of ages using an analysis of the probability distribution of all grain ages; this method derives an age of 2.86 ± 0.02 Ma for the youngest group, consisting of 17 analyses. Last, an algorithm in Isoplot (freely available from the Berkeley Geochronology Center at http://www.bgc.org/isoplot_etc/isoplot.html) that searches for the youngest group of analyses while taking into account anomalous results such as those with high common Pb, yields an age of 2.85 ± 0.06 Ma. All of these methods treat each analysis equally, whereas we specifically targeted some grains with multiple analyses and we also targeted cores of grains. Eight of the 14 analyzed cores yielded ages older than 3.0 Ma, one of which had high common Pb (>6%), as did one of the six cores with ages younger than 3.0 Ma. If we use only the young group of analyses that came from outer parts of grains (table 2), the weighted mean age for the youngest eight is 2.72 ± 0.03 Ma; that for the youngest 10 analyses is 2.78 ± 0.02 Ma. Each method of analysis has its merits. We favor the approach that ignores the inner parts of zircon grains, while acknowledging the methods that use all of the analyses. We thus interpret the age of the dacite to be 2.8 ± 0.03 Ma.

The six oldest zircon ages (table 2), most of them from cores of grains but one representing an outer part, are within 1 σ of the K-Ar plagioclase age of 4.4 ± 1.1 Ma; all others are significantly younger. This result was unexpected because plagioclase would be expected to be degassed while in the hot lava, and yield an age at the young end of the zircon age spectrum. However, all zircon ages lie within 2 σ of the K-Ar age and are compatible at 95% certainty.

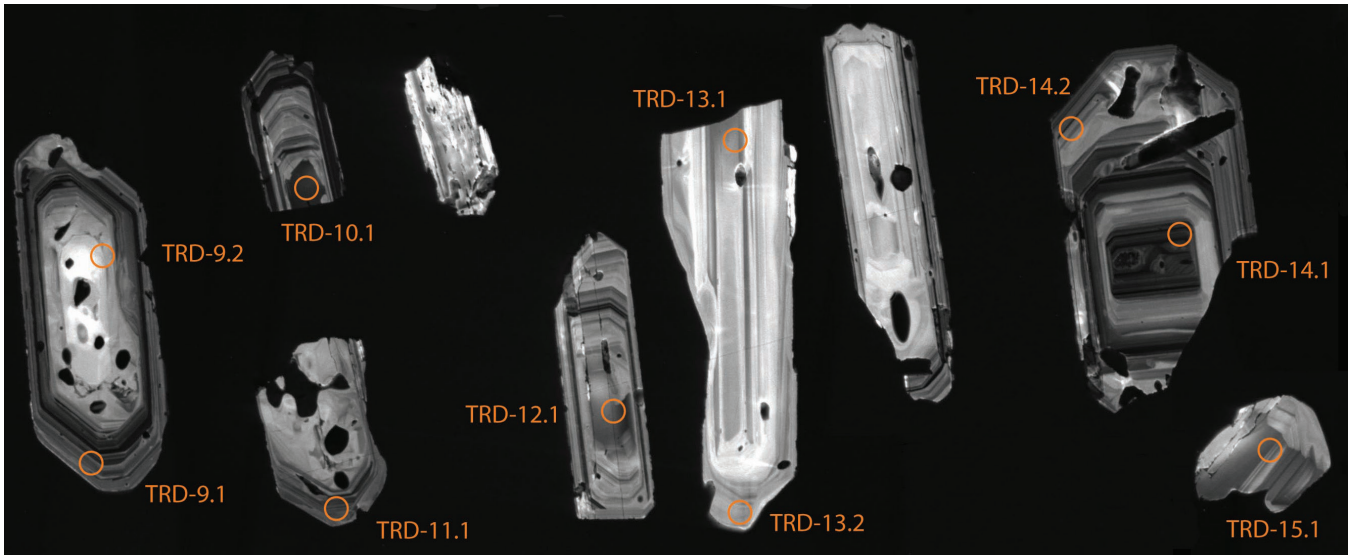

Figure 8. *Cathode luminescence image of a subset of analyzed zircon grains from the Wildcat Hills dacite (Tdw), sample number F06_371CV. Circles represent analysis sites before burning the spot on the grain, and are 20 microns in diameter. Labels correspond to value in Spot Name field (table 2).*

Table 2. *Data used to calculate the U-Pb age of Wildcat Hills dacite unit (sample F06_371CV).*

Spot Name	Spot Position in grain*	Common ^{206}Pb (%)	U (ppm)	Th (ppm)	^{232}Th/^{238}U	207 corrected ^{206}Pb/^{238}U age (Ma)	Error (1 s)
TRD-6.1	o	2.51	305.2	162.4	0.55	2.63	0.08
TRD-9.1	o	0.99	900.6	482.3	0.55	2.65	0.04
TRD-5.1	o	0.75	878.7	407.6	0.48	2.66	0.05
TRD-8.1	o	5.30	210.4	126.3	0.62	2.67	0.10
TRD-28.2	c	1.08	1273.7	705.3	0.57	2.69	0.04
TRD-7.2	o	2.53	725.9	1374.5	1.96	2.74	0.05
TRD-14.2	o	1.69	503.8	260.8	0.53	2.75	0.06
TRD-9.2	c	8.97	72.4	50.6	0.72	2.75	0.18
TRD-23.1	i	1.02	1506.0	764.7	0.52	2.77	0.04
TRD-22.1	c	4.33	272.7	145.6	0.55	2.78	0.09
TRD-3.2	o	1.67	1712.0	694.3	0.42	2.79	0.04
TRD-18.1	i	0.76	1785.4	1024.3	0.59	2.80	0.03
TRD-25.1	i	1.45	768.1	1014.4	1.36	2.81	0.05
TRD-19.1	c	2.60	3994.0	1461.4	0.38	2.81	0.02
TRD-7.1	i	3.21	506.1	851.5	1.74	2.82	0.07
TRD-15.1	c	2.65	230.7	238.4	1.07	2.91	0.10
TRD-16.1	c	0.75	1791.7	988.0	0.57	2.93	0.03
TRD-26.1	o	3.06	159.6	94.7	0.61	2.94	0.12
TRD-11.1	i	18.51	631.9	299.1	0.49	2.93	0.20
TRD-4.1	o	1.48	293.1	159.1	0.56	3.01	0.09
TRD-21.1	o	1.64	1149.8	306.9	0.28	3.01	0.04
TRD-6.2	c	9.63	63.3	58.2	0.95	3.04	0.18
TRD-4.2	c	5.22	135.8	79.0	0.60	3.05	0.13
TRD-13.1	i	12.51	160.2	194.5	1.25	3.05	0.12
TRD-2.1	i	0.97	1507.3	836.6	0.57	3.10	0.04
TRD-20.1	o	0.33	848.6	449.9	0.55	3.12	0.05
TRD-13.2	o	5.19	158.5	94.6	0.62	3.14	0.12
TRD-1.1	i	3.54	235.5	192.7	0.85	3.20	0.10
TRD-8.2	c	2.12	111.4	101.8	0.94	3.21	0.14
TRD-10.1	c	1.73	320.4	340.1	1.10	3.26	0.08
TRD-14.1	c	0.72	1831.8	766.0	0.43	3.33	0.03
TRD-12.1	c	2.29	482.7	827.8	1.77	3.43	0.07
TRD-17.1	c	1.06	592.7	599.8	1.05	3.54	0.07
TRD-24.1	o	1.01	2010.1	1148.8	0.59	3.58	0.04
TRD-3.1	c	0.80	21793.4	16563.7	0.79	4.31	0.03

Notes:
* c=core, i=indeterminate, o=outer
Data sorted by age (Ma).
Zircons with multiple analyses have same Spot Name prefix (e.g., TRD-6.1 and TRD-6.2).
Sample analyzed by D. Miller at the SHRIMP-RG laboratory, Stanford University, Palo Alto, California.

^{40}Ar/^{39}Ar Data

The Wildcat Hills rhyolite (Qrw) also was a top priority for reanalysis. Smith and others (1978) reported a K-Ar sanidine age of 3.1 ± 0.5 Ma for the unit, or 3.2 Ma when recalculated using the decay constants of Steiger and Jager (1977). Miller and others (1995) obtained a K-Ar sanidine age of 2.1 ± 0.1 Ma for sample M93WI-40 (table 1, plate 1). Miller and others (1995) described several possible reasons for the disparity between the two ages, and after a thorough review of the analytical data for both samples, concluded that their younger age was more valid. In an attempt to resolve the discrepancy, we reanalyzed the unit using ^{40}Ar/^{39}Ar techniques. Sample F06_306CV (table 1, plate 1) was collected from the same outcrop as M93WI-40, and yielded an ^{40}Ar/^{39}Ar sanidine age of 2.331 ± 0.010 Ma (table 3, figure 10) which is slightly older, but in general agreement (at 2 σ) with the age of Miller and others (1995).

Previously undated basalt flows north of the Wildcat Hills and northeast of Cedar Hill (figure 1) were outside of the quadrangles, but were considered to represent important parts of the eruptive history of the area. ^{40}Ar/^{39}Ar analysis of groundmass yielded an age of 2.238 ± 0.022 Ma for the flows north of the Wildcat Hills (sample F06_098CV, tables 1 and 3, figures 1 and 11), and 0.521 ± 0.017 Ma for the flows northeast of Cedar Hill (sample F06_437CV, tables 1 and 3, figures 1 and 12).

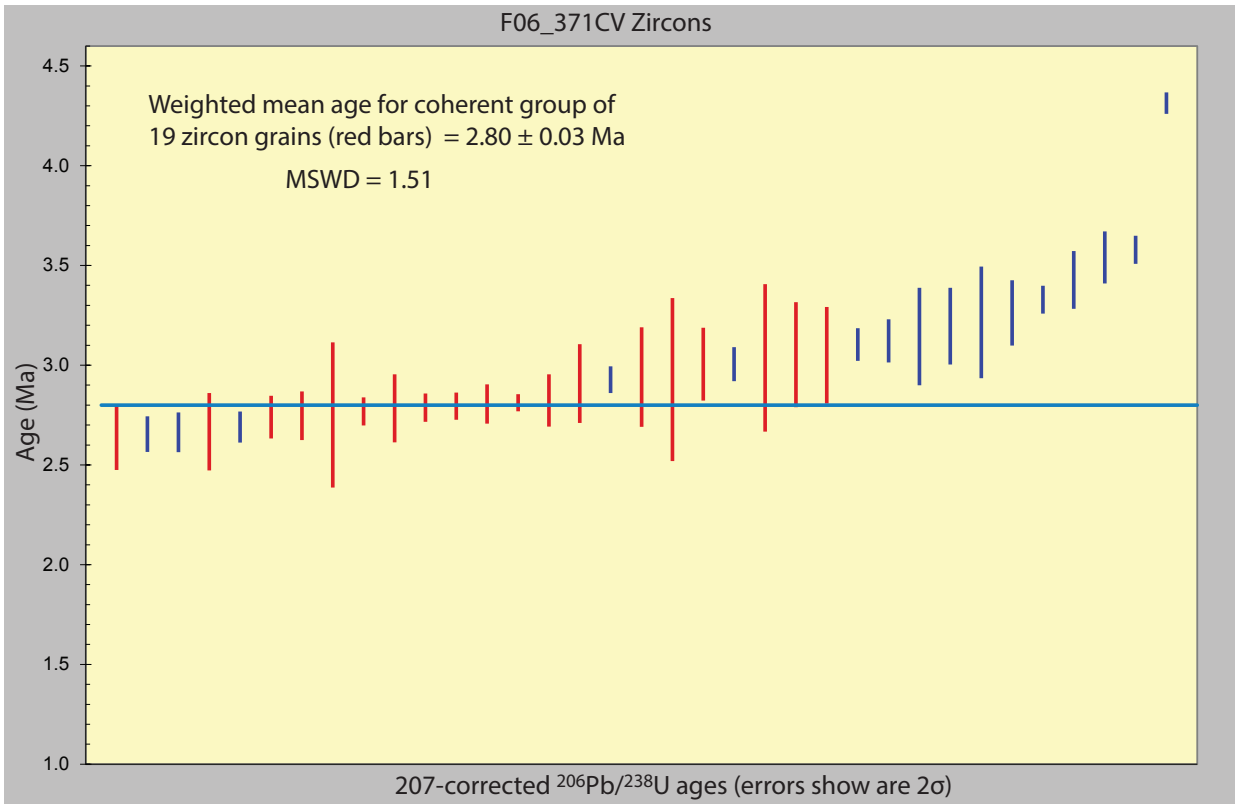

Figure 9. *Plot of 207-corrected $^{206}Pb/^{238}U$ ages (Ma) for zircons from the Wildcat Hills dacite (Tdw), sample number F06_371CV. Red bars are analyses used to calculate weighted mean age.*

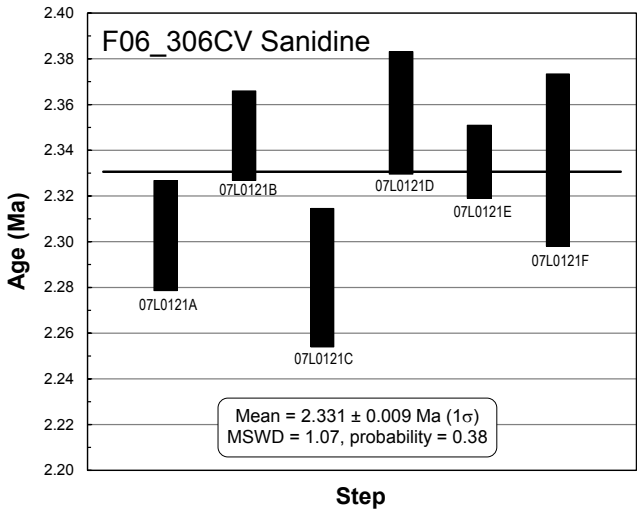

Figure 10. *Data used to calculate weighted mean age (heavy black line) of sanidine from the Rhyolite of Wildcat Hills (Qrw), sample number F06_306CV (table 3).*

Comparison of Radiometric Ages and Geomagnetic Timescale

New aeromagnetic data provide a source of indirect age information for the volcanic units. We compared the radiometric age of each volcanic unit (table 1) with the geomagnetic timescale of Cande and Kent (1995) to determine whether the radiometric age corresponded to a normal or reversed polarity event (figure 13). The outcrop distribution of each unit was then compared to the aeromagnetic data (figures 4, 5, and 7) to determine whether the associated anomalies were positive or negative. A positive (high) anomaly indicates the unit erupted during a normal polarity event, while a negative (low) anomaly indicates the unit erupted during a reversed polarity event. In general the radiometric ages were consistent with the polarity indicated by the aeromagnetic data.

The middle Pleistocene basalt (Qb) at Cedar Hill and Middle Shield (plate 1, figure 1) corresponds to strong positive magnetic anomalies (figures 4, 5, and 7). The K-Ar whole-rock age of 1.16 ± 0.08 Ma for Cedar Hill (table 1) is within the Matuyama reversed chron (0.78 to 2.581 Ma; Cande and Kent, 1995) (figure 13); however, this reversed polarity time was punctuated by times of normal polarity. The K-Ar age does overlap within the uncertainty of 1 σ, and therefore could have been erupted during the normal Cobb Mountain subchron (1.19 to 1.215 Ma; Channell and others, 2002). The K-Ar whole-rock age of 0.72 ± 0.15 Ma for Middle Shield (table 1) is within the Brunhes normal polarity chron (figure 13), precluding the older end of the age uncertainty, which would place the age within a reversed polarity chron. Most of the other outcrops of basalt in eastern Curlew Valley also correspond to positive magnetic anomalies (figures 1 and 7). The middle Pleistocene flows (Qb) north of Cedar Hill and at Locomotive Springs Shield (figure 1) have ages of 0.521 ± 0.017

Table 3. *Analytical data for new $^{40}Ar/^{39}Ar$ ages for volcanic rocks in and adjacent to the Kelton Pass SE and Monument Peak SW quadrangles.*

F06_306CV Sanidine IRR246-49 J (converted) = 0.0003321577±0.0000005721 (Converted to FCT Age = 28.02 Ma)

Step Incl. in Mean	mol $^{39}Ar_K$	% $^{39}Ar_K$ Released	% ^{40}Ar*	^{40}Ar (Volts±uVolts)	^{39}Ar (Volts±uVolts)	^{38}Ar (Volts±uVolts)	^{37}Ar (Volts±uVolts)	^{36}Ar (Volts±uVolts)	K/Ca	K/Cl	Age (Ma)
07L0121A	2.391E-15	16.3968	98.854	0.378131±774	0.097209±197	0.001321±33	0.001189±319	0.000015±13	42.904	5425.1	2.303 ± 0.024
07L0121B	2.928E-15	20.0749	101.415	0.459805±937	0.119014±241	0.001591±40	0.001322±302	0.000000±12	47.247	6758.9	2.346 ± 0.020
07L0121C	1.949E-15	13.3632	88.479	0.341550±701	0.079224±161	0.001090±38	0.000726±265	0.000133±13	57.227	6381.1	2.284 ± 0.030
07L0121D	2.096E-15	14.3708	101.792	0.329340±677	0.085198±173	0.001158±35	0.001427±223	0.000000±12	31.317	4987.1	2.356 ± 0.027
07L0121E	3.794E-15	26.0153	95.252	0.631360±1280	0.154231±311	0.002068±46	0.001452±255	0.000102±13	55.735	8375.9	2.335 ± 0.016
07L0121F	1.426E-15	9.7791	100.432	0.225151±469	0.057975±119	0.000797±31	0.000418±274	0.000000±12	72.856	4363.3	2.336 ± 0.038
						Wtd Mean Age (Ma), N = 6			**MSWD = 1.067**		**2.331 ± 0.010**
						Isochron Age (Ma)					none
						Integrated Age (Ma)					2.328 ± 0.016

F06_098CV Groundmass IRR275-20 J (converted) = 0.0003306453±0.0000005571 (Converted to FCT Age = 28.02 Ma)

Step (°C)	mol $^{39}Ar_K$	% $^{39}Ar_K$ Released	% ^{40}Ar*	^{40}Ar (Volts±uVolts)	^{39}Ar (Volts±uVolts)	^{38}Ar (Volts±uVolts)	^{37}Ar (Volts±uVolts)	^{36}Ar (Volts±uVolts)	K/Ca	K/Cl	Age (Ma)
550	4.299E-15	21.9267	14.179	3.987930±8025	0.156648±316	0.004463±38	0.210773±1021	0.011641±33	0.390	2296.8	2.154 ± 0.063
600	3.433E-15	17.5102	18.173	2.702009±5476	0.126258±254	0.003193±29	0.319309±1162	0.007572±25	0.207	3095.2	2.323 ± 0.055
650	2.825E-15	14.4108	22.416	1.755034±3582	0.103189±208	0.002319±28	0.471321±1578	0.004740±21	0.115	3420.0	2.280 ± 0.049
700	2.470E-15	12.5993	29.275	1.172325±2417	0.091150±184	0.001841±24	0.655027±2467	0.002990±18	0.073	2848.7	2.256 ± 0.043
750	1.985E-15	10.1267	36.577	0.730550±1534	0.073384±148	0.001345±24	0.699006±2830	0.001764±15	0.055	3196.1	2.186 ± 0.040
825	2.165E-15	11.0437	39.248	0.699571±1472	0.079473±160	0.001411±24	0.916801±1887	0.001696±15	0.045	3217.6	2.077 ± 0.038
900	1.261E-15	6.4314	33.942	0.459475±997	0.046320±123	0.000915±20	0.587076±2953	0.001192±14	0.041	1683.7	2.026 ± 0.058
975	5.480E-16	2.7950	13.035	0.316623±790	0.020140±54	0.000576±19	0.269552±1440	0.001008±13	0.039	618.3	1.234 ± 0.123
1050	3.378E-16	1.7231	11.282	0.295283±737	0.012464±106	0.000479±53	0.233202±2703	0.000952±30	0.028	355.5	1.615 ± 0.452
1150	2.810E-16	1.4331	3.589	0.654945±1353	0.011163±35	0.001300±32	1.316891±3339	0.002507±19	0.004	60.4	1.370 ± 0.354
						Wtd Mean Plateau age (Ma)			**MSWD = 1.7**		**2.238 ± 0.022**
				Intercept = 295.9±9.8		Isochron age (Ma)			MSWD = 3.2		2.231 ± 0.274
						Integrated age (Ma)					2.155 ± 0.022

F06_437CV Groundmass IRR246-50 J (converted) = 0.0003283521±0.0000005652 (Converted to FCT Age = 28.02 Ma)

Step (°C)	mol $^{39}Ar_K$	% $^{39}Ar_K$ Released	% ^{40}Ar*	^{40}Ar (Volts±uVolts)	^{39}Ar (Volts±uVolts)	^{38}Ar (Volts±uVolts)	^{37}Ar (Volts±uVolts)	^{36}Ar (Volts±uVolts)	K/Ca	K/Cl	Age (Ma)
550	1.889E-16	0.9303	-4.079	0.066787±251	0.007702±47	0.000149±22	0.031739±1940	0.000244±16	0.127	5328.6	-0.210 ± 0.357
625	1.588E-15	7.8196	5.380	0.677159±1459	0.064733±132	0.001369±37	0.253321±2237	0.002239±21	0.134	2123.4	0.334 ± 0.062
700	4.811E-15	23.6896	11.821	1.392801±2889	0.196037±397	0.003493±42	0.664923±2969	0.004343±28	0.154	4255.5	0.499 ± 0.029
775	5.606E-15	27.6050	13.022	1.559060±3222	0.228481±462	0.003916±44	0.836044±3246	0.004824±30	0.143	8131.8	0.528 ± 0.027
850	3.040E-15	14.9676	8.926	1.339354±2714	0.123997±251	0.002533±44	0.612187±2996	0.004300±26	0.106	3243.3	0.573 ± 0.042
925	1.938E-15	9.5413	3.996	1.605564±3246	0.079033±161	0.002226±43	0.375675±2522	0.005322±32	0.110	1450.9	0.482 ± 0.082
1000	1.609E-15	7.9239	1.296	2.724571±5484	0.066401±136	0.003767±53	1.390089±5247	0.009491±36	0.025	236.9	0.320 ± 0.129
1075	1.227E-15	6.0433	2.807	1.969735±3974	0.051715±106	0.002400±49	2.571416±5806	0.007201±34	0.010	458.3	0.656 ± 0.141
1175	7.677E-17	0.3780	-7.567	0.229203±519	0.003186±44	0.000224±23	0.092179±1561	0.000860±18	0.018	539.9	-3.295 ± 1.323
1400	2.237E-16	1.1013	-9.455	0.636515±1331	0.009110±92	0.000662±29	0.025903±1471	0.002365±25	0.184	375.8	-3.925 ± 0.796
						Wtd Mean Plateau age (Ma)			**MSWD = 1.15**		**0.521 ± 0.017**
				Intercept = 294.6±2.3		Isochron age (Ma)			MSWD = 1.6		0.536 ± 0.051
						Integrated age (Ma)					0.429 ± 0.020

Notes:
All samples analyzed by R. Fleck at the U.S. Geological Survey geochronology laboratory in Menlo Park, CA. Samples shown with temperature steps (437F06CV and 98F06CV) were analyzed by $^{40}Ar/^{39}Ar$ incremental heating analysis. *Plateau* ages are reported only if present according to the definition of Fleck and others (1977). Samples whose steps are not temperature increments (F06_306CV) were analyzed by single-step, $^{40}Ar/^{39}Ar$ laser-fusion analysis. The *weighted mean age* and number (*N*) of selected samples is reported. For either type of analysis, an *Integrated age* is calculated as the age of Ar released in all steps; an *Isochron* age is calculated by least squares regression (York, 1969) of selected steps of the Parent-Daughter isotope co-variation. The age interpreted to best represent the age of that sample is shown in **boldface** type.

Ma and 0.44 ± 0.1 Ma, respectively (table 1); both ages are entirely within the Brunhes normal polarity chron (figure 13).

The early Pleistocene basalt (Qb) exposed along the Coyote Spring fault in central Curlew Valley (figure 1) is associated with a weak magnetic low (figure 7), consistent with its $^{40}Ar/^{39}Ar$ groundmass age of 2.238 ± 0.022 Ma (tables 1 and 3), entirely within the Matuyama reversed polarity chron (figure 13). Similarly, outcrops of the Wildcat Hills rhyolite (Qrw) (plate1) coincide with magnetic lows (figures 4 and 5), consistent with the $^{40}Ar/^{39}Ar$ sanidine age of 2.331 ± 0.010 Ma (tables 1 and 3), which also lies entirely within the Matuyama reversed polarity chron (figure 13).

The Wildcat Hills dacite (Tdw) (plate 1) coincides with both positive and negative magnetic anomalies (figures 4 and 5). The dacite exposed in the eastern Wildcat Hills coincides with positive magnetic anomalies, with the highest values located over the southern part of the hill (figures 4 and 5). The normal polarity of these anomalies is consistent with the U-Pb zircon age of 2.8 ± 0.03 Ma (tables 1 and 2), which is entirely within the Gauss normal polarity chron (2.581 to 3.58 Ma; Cande

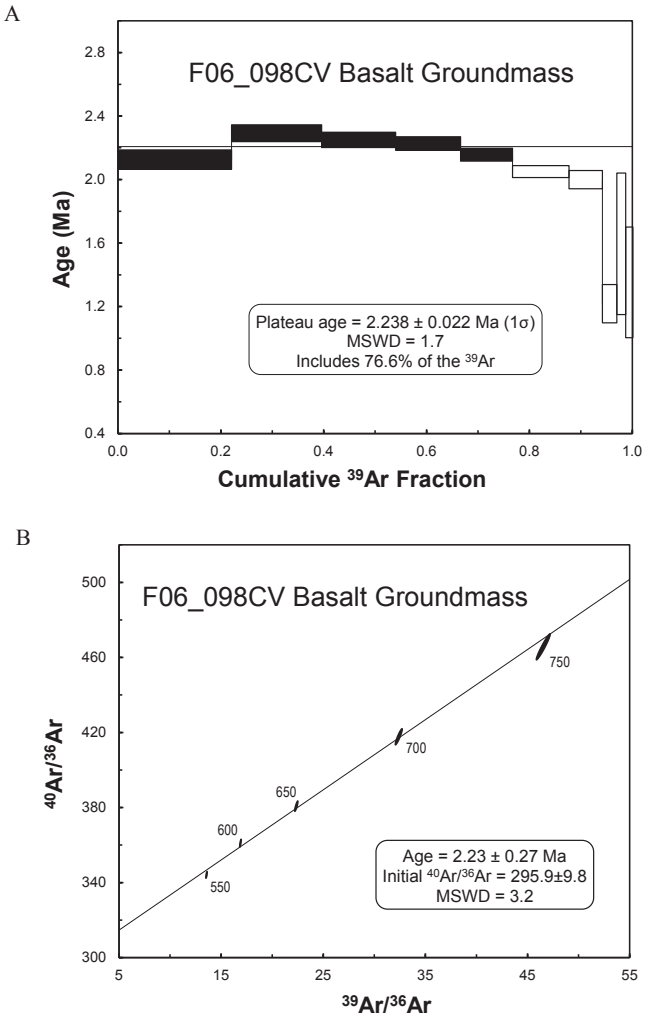

Figure 11. A. *Age spectrum plot for basalt groundmass, sample F06_098CV. Plateau age calculated using methodology of Fleck and others (1977). Temperature steps used to calculate plateau age are shown as black bars, and are highlighted in boldface type in table 3.* ***B.*** *Isochron age for same sample and temperature steps.*

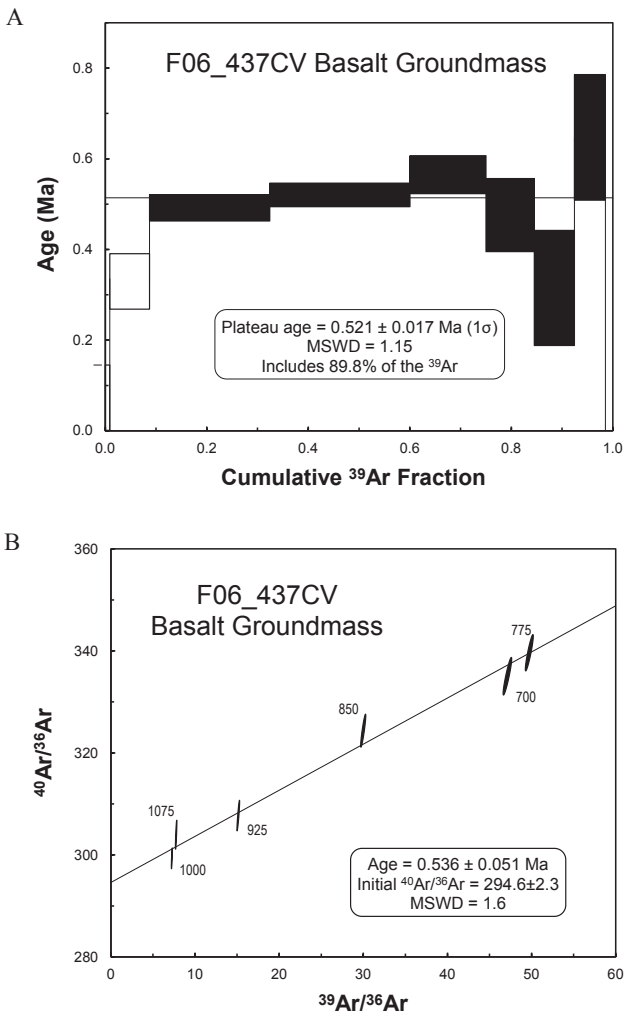

Figure 12. A. *Age spectrum plot for basalt groundmass, sample F06_437CV. Plateau age calculated using methodology of Fleck and others (1977). Temperature steps used to calculate plateau age are shown as black bars, and are highlighted in boldface type in table 3.* ***B.*** *Isochron age for same sample and temperature steps.*

and Kent, 1995) (figure 13). The more discontinuous exposures to the southeast, however, coincide with magnetic lows, suggesting that these may be of a distinctly different age, and that the dacite erupted over several hundred thousand years. This hypothesis is supported by the zircon data (table 2) in that a majority of the zircon determinations are consistent with eruption of the dacite (Tdw) during the Gauss normal chron. However, three of the ages lie in the Kaena reversed subchron (3.040 to 3.110 Ma; Cande and Kent, 1995), two lie in the Mammoth reversed subchron (3.220 to 3.330 Ma; Cande and Kent, 1995), and the oldest age of 4.3 Ma is in the Gilbert reversed polarity chron (3.58 to 5.894 Ma; Cande and Kent, 1995). Three generations of plagioclase, and possibly two generations of pyroxene (Shea, 1985), are present in the dacite (Tdw) flows and may be further evidence that the magmatic system was active for a long period of time.

The Pliocene basaltic lava flows (Tb) south of Wildcat Hills (plate 1) coincide with very subtle magnetic anomalies (<1-2 nT; figures 4 and 5). The two ages for this unit (table 1) span a magnetization boundary, with a slight magnetic low coinciding with the northern age (3.6 ± 0.1 Ma) and a slight magnetic high coinciding with the southern age (4.9 ± 0.4 Ma). The uncertainty of the southern age spans multiple polarity chrons, but the northern age would be consistent with its having been erupted at 3.58 Ma or later during a reversed chron (figure 13).

VOLCANISM

Volcanic rocks within the map area are exposed in and south of the Wildcat Hills, and east of Deep Creek at Cedar Hill and Middle Shield (plate 1, figure 1). Rocks in the Wildcat Hills are bimodal (table 4, figure 14) and include Pliocene basaltic lava flows (Tb) with K-Ar ages of 4.9 and 3.6 Ma, the Wildcat Hills dacite (Tdw) with a U-Pb age of 2.8 ± 0.03 Ma, and the Wildcat Hills rhyolite (Qrw) with an $^{40}Ar/^{39}Ar$ sanidine age

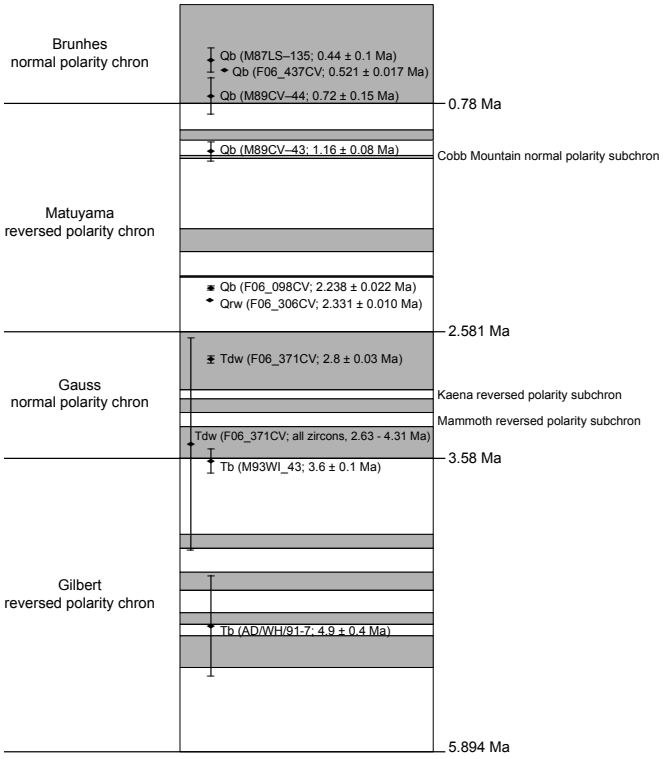

Figure 13. *Comparison of radiometric ages of volcanic units in and adjacent to the Kelton Pass SE and Monument Peak SW quadrangles with the geomagnetic timescale of Cande and Kent (1995). Normal polarity intervals are shaded in gray; reversed polarity intervals are white. Radiometric age and associated error shown as black diamond with bracketed line. Errors for samples F06_437CV and F06_306CV are too small to depict.*

of 2.331 ± 0.010 Ma (plate 1, table 1). Basalt flows (Qb) at Cedar Hill and Middle Shield have K-Ar whole rock ages of 1.16 and 0.72 Ma, respectively (figure 1, table 1). A hiatus of about one million years separates the Pliocene and early Pleistocene bimodal eruptive sequence in the Wildcat Hills from the younger Pleistocene basalts to the east, which represent the youngest extension-related volcanism in the map area, as well as in northern Utah (Miller and others, 1995). The alignment of the vents that produced the bimodal lavas in central Curlew Valley, and the Pleistocene basalt (Qb) in eastern Curlew Valley (figure 1) is roughly parallel to the structural grain of the area, suggesting that faults influenced the location of the vent systems.

New $^{40}Ar/^{39}Ar$ data for previously undated basalts north of the Wildcat Hills and northeast of Cedar Hill provide important insights into the eruptive history of the greater Curlew Valley area. The basalt north of the Wildcat Hills yielded an $^{40}Ar/^{39}Ar$ groundmass age of 2.238 ± 0.022 Ma (table 1, figure 1), which is slightly younger than, but generally coeval with the Wildcat Hills rhyolite (Qrw). Although a single long-lived eruptive center is possible, there may be two distinct episodes of bimodal volcanism recorded in the Wildcat Hills—one that produced the Pliocene basaltic lavas (Tb) and dacite (Tdw) (4.9–2.8 Ma), and a second episode that produced the Wildcat Hills rhyolite (Qrw) and the basalt flows (Qb) (2.3–2.2 Ma) associated with the Coyote Spring fault (figure 1). The basalt northeast of Cedar Hill yielded an $^{40}Ar/^{39}Ar$ groundmass age of 0.521 ± 0.017 Ma (table 1, figure 1). Miller and others

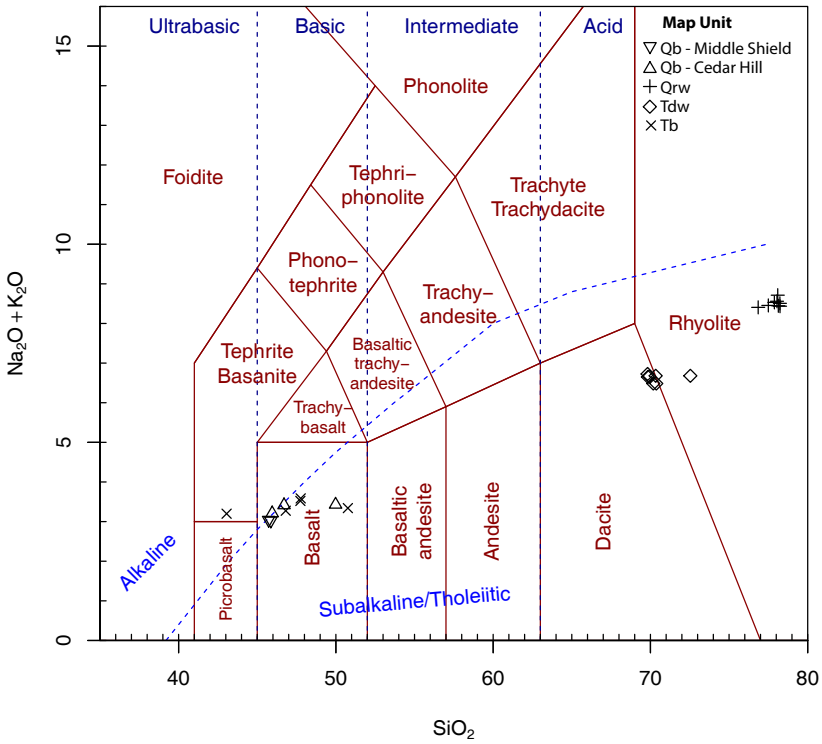

Figure 14. *Total alkali-silica plot (after LeBas and others, 1986) of Tertiary and Quaternary lava flows in the Kelton Pass SE and Monument Peak SW quadrangles. Plot generated from major-element whole-rock geochemistry data (table 4) using the GeoChemical Data Toolkit (GCDKit) of Janoušek and others (2006).*

Table 4. *Major-element whole-rock geochemistry data for volcanic units in Kelton Pass SE and Monument Peak SW quadrangles.*

Sample Number	MapUnit	Rock Name	7.5' Quadrangle	Latitude (N)	Longitude (W)	SiO_2	TiO_2	Al_2O_3	Fe_2O_3T	MnO	MgO	CaO	Na_2O	K_2O	P_2O_5	Total	TOTALa	Reference
M87LS-136	Qb	Basalt	Monument Peak SW	41.777251	-112.951348	45.37	3.04	14.07	15.70	0.21	6.92	10.71	2.39	0.63	0.96	100.00	99.19	Miller and others (1995)
M89CV-43	Qb	Basalt	Monument Peak	41.840199	-112.859982	45.40	3.15	14.18	16.06	0.22	6.71	10.11	2.53	0.64	1.00	100.00	100.89	Miller and others (1995)
M87LS-139	Qb	Basalt	Locomotive Springs	41.747112	-112.903896	45.40	3.05	14.17	15.87	0.21	7.08	10.28	2.40	0.59	0.95	100.00	100.66	Miller and others (1995)
PV83-20	Qb	Basalt	Monument Peak	41.848300	-112.864024	46.11	2.89	14.60	15.52	0.20	6.75	9.75	2.68	0.69	0.81	100.00	98.47	Kerr (1987)
RS-8373	Qb	Basalt	Monument Peak SW	41.817993	-112.880820	49.37	2.79	15.79	12.84	0.20	6.81	8.57	2.76	0.63	0.24	100.00	99.94	Shea (1985)
M91CV-91	Qb?	Basalt	Monument Peak SW	41.765492	-112.880068	45.69	3.00	14.87	15.56	0.21	6.87	9.64	2.48	0.78	0.89	100.00	100.90	Miller and others (1995)
M93WI-40	Qrw	Rhyolite	Kelton Pass SE	41.845317	-113.025920	76.85	0.12	12.26	1.14	0.03	0.12	1.01	3.09	5.32	0.05	100.00	99.44	Miller and others (1995)
RS-OBS-1	Qrw	Rhyolite	Kelton Pass SE	41.843904	-113.020690	77.46	0.20	11.48	0.91	0.00	0.33	1.15	3.20	5.25	0.02	100.00	100.54	Shea (1985)
RS-8394	Qrw	Rhyolite	Kelton Pass SE	41.850476	-113.018393	77.86	0.20	11.72	0.89	0.01	0.12	0.62	3.15	5.38	0.04	100.00	99.41	Shea (1985)
RS-8398	Qrw	Rhyolite	Kelton Pass SE	41.849293	-113.036789	77.96	0.20	11.47	1.08	0.01	0.06	0.64	3.22	5.33	0.02	100.00	100.61	Shea (1985)
RS-83101	Qrw	Rhyolite	Kelton Pass SE	41.834833	-113.033028	78.09	0.20	11.48	0.86	0.01	0.00	0.62	3.36	5.35	0.02	100.00	99.78	Shea (1985)
RS-8392	Qrw	Rhyolite	Kelton Pass SE	41.832589	-113.039541	78.11	0.20	11.63	0.93	0.01	0.00	0.64	3.22	5.22	0.03	100.00	99.35	Shea (1985)
RS-8391	Qrw	Rhyolite	Kelton Pass SE	41.836592	-113.052832	78.21	0.09	11.51	0.88	0.01	0.17	0.60	3.10	5.40	0.01	100.00	97.96	Shea (1985)
RS-8393	Qrw	Rhyolite	Kelton Pass SE	41.831458	-113.030176	78.22	0.20	11.61	0.88	0.01	0.00	0.60	3.04	5.40	0.04	100.00	99.47	Shea (1985)
M93WI-34	Tdw	Dacite	Monument Peak SW	41.849361	-112.992210	69.82	0.49	14.29	3.71	0.06	1.31	3.47	3.27	3.46	0.12	100.00	99.60	Miller and others (1995)
M93WI-37	Tdw	Dacite	Kelton Pass SE	41.852431	-113.014387	69.84	0.51	14.35	3.72	0.06	1.26	3.49	3.31	3.35	0.12	100.00	99.40	Miller and others (1995)
L93WI-14	Tdw	Dacite	Kelton Pass SE	41.857421	-113.000260	69.93	0.49	14.17	3.74	0.06	1.39	3.43	3.21	3.45	0.13	100.00	99.63	Miller and others (1995)
RS-8454	Tdw	Dacite	Kelton Pass SE	41.854059	-113.013722	69.96	0.55	14.27	3.95	0.06	1.62	3.09	3.13	3.34	0.04	100.00	102.55	Shea (1985)
RS-8376	Tdw	Dacite	Curlew Junction	41.885127	-113.006694	70.27	0.67	14.26	3.36	0.05	1.49	3.33	3.39	3.08	0.09	100.00	100.86	Shea (1985)
M93WI-33	Tdw	Dacite	Monument Peak SW	41.847701	-112.991100	70.34	0.51	14.09	3.68	0.06	1.26	3.27	3.33	3.34	0.12	100.00	99.69	Miller and others (1995)
RS-83103	Tdw	Rhyolite	Monument Peak SW	41.846374	-112.996677	72.49	0.49	13.71	2.86	0.03	0.92	2.76	3.21	3.47	0.06	100.00	100.36	Shea (1985)
M93WI-43	Tb	Basalt	Kelton Pass SE	41.817184	-113.031202	46.81	3.04	14.77	16.07	0.21	6.15	9.24	2.54	0.74	0.43	100.00	100.20	Miller and others (1995)
PV83-3	Tb	Basalt	Kelton Pass SE	41.821457	-113.028613	47.13	2.92	15.12	15.65	0.19	5.88	9.20	2.93	0.61	0.37	100.00	98.54	Kerr (1987)
PV83-28	Tb	Basalt	Kelton Pass SE	41.813861	-113.034297	47.15	2.97	14.85	15.75	0.20	6.13	9.09	2.73	0.75	0.37	100.00	99.49	Kerr (1987)
RS-83910	Tb	Basalt	Kelton Pass SE	41.818566	-113.031228	50.23	2.70	16.17	12.92	0.20	5.48	8.82	2.68	0.62	0.17	100.00	99.73	Shea (1985)
F07_253CV	Tb?	Tephrite-Basanite	Kelton Pass SE	41.787116	-113.058559	43.05	4.37	12.95	19.37	0.25	5.86	9.88	2.41	0.79	1.06	100.00	98.81	Miller and others (in prep.)

Notes:

Location data in NAD83.

Major oxides reported in weight percent, normalized to 100% on a volatile free basis.

Data for each map unit are sorted by increasing SiO_2 value.

Rock names derived from total alkalai-silica diagram of LeBas and others (1986), shown in figure 10.

TOTALa = Analytical total.

Fe_2O_3T = Total iron as Fe_2O_3.

Samples numbers from Shea (1985) have been given an "RS-" prefix for the purpose of this study.

(1995) observed that the basalt shield volcanoes of eastern Curlew Valley decreased systematically in age and size southward (table 1, figure 1), with a new volcano forming about every 300,000 to 400,000 years. While the age for the basalt flows northeast of Cedar Hill reinforces that young basalts are restricted to the east side of the valley, the age is most similar to the southernmost dated basalt that forms Locomotive Springs Shield and has an age of 0.44 ± 0.1 Ma (table 1, figure 1). Therefore it does not fit the proposed sequence, indicating that the spatial and temporal progression of eruptions is not as systematic and straightforward as previously thought.

The new aeromagnetic data provide insights into the presence and extent of volcanic units in the subsurface. A positive aeromagnetic anomaly lies along the west edge of the Hansel Mountains (figures 1 and 7) coinciding in places with small, non-contiguous outcrops of basalt east of Middle Shield (plate 1; Qb?) and Cedar Hill (figure 1; Qb). The anomaly indicates the presence of basalt in the subsurface, and the polarity and continuity of the anomaly to Cedar Hill suggests it may represent flows that erupted from Cedar Hill and pooled against the fault-controlled west side of the Hansel Mountains. The areas covered by Quaternary deposits (Qs) adjacent to the basalt shields and north of the map area along Deep Creek (figure 1) are underlain mostly by magnetic lows and some subtle highs (figure 7). The magnitude and polarity of the anomalies are generally similar to those associated with the early Pleistocene basalt (Qb) exposed along the Coyote Spring fault (figure 1). Based on these similarities, and the proximity of outcrops of Quaternary basalt, we infer that the anomalies are indicative of older Quaternary basalt flows. It is possible, however, that Tertiary basalt flows are also present. Basalt flows in the upper 600 feet (180 m) of the Government-Gabrielson, and Federal No. 1 and No. 2 exploration wells (Peace, 1956), east of the Coyote Spring fault (figure 1) are inferred to be Tertiary age because they are interbedded with tuffaceous sedimentary rocks that are likely Salt Lake Formation (Ts).

The Wildcat Hills rhyolite (Qrw) is underlain by two oblong lows delineated by magnetization boundaries (figures 4 and 5) that may reflect vent areas (plate 1). One of these lows underlies the topographically highest rhyolite outcrops, which had been identified from map data as a vent area (this study; Howes, 1972). The three highest outcrop areas of rhyolite are aligned approximately along the Coyote Spring fault (plate 1), and may represent individual conduits that fed the eruption. Flow foliation and lineation data suggest that the bulk of the rhyolite flowed from this vent area to the northwest, and a smaller lobe flowed to the east (plate 1). The other low underlies the northwesternmost oval-shaped outcrop area. Prior to availability of the new aeromagnetic data, these outcrops were considered to be part of the lobe that had flowed to the northwest from the vent area described above. Field observations for the northwest outcrops and the boundary between the two outcrop areas were reexamined in light of the magnetic data. Unfortunately, only one field traverse intersected the boundary between the two outcrop areas, so data are lacking in critical areas; however, the existing flow foliation data could support the presence of a vent under the northwest outcrops (plate 1). Interestingly, the topographic profile of the northwest outcrops is generally flat-lying, whereas outcrops to the southeast have a profile that slopes about five degrees to the northwest (plate 2; B-B′). The difference in topographic profiles between the two outcrop areas might be further evidence that the rhyolite (Qrw) erupted from two vent areas. Subtle magnetic highs and lows of limited lateral extent underlie the rhyolite (Qrw) outcrops in the area between the two proposed vents (figures 4 and 5). These anomalies are similar to those associated with outcrops of Tertiary basalt (Tb) south of the Wildcat Hills. Inclusions of inferred Tertiary basalt (Tb) are present in both the rhyolite (Qrw) and dacite (Tdw), so we infer that at least several of the magnetic anomalies underlying the rhyolite (Qrw) are attributable to Tertiary basalt (Tb). Similar anomalies underlying Quaternary surficial deposits around the northwest outcrops of rhyolite (Qrw) and west and southwest of the Oquirrh Formation (Pos) outcrops are also thought to reflect Tertiary basalt (Tb).

Outcrops of the Wildcat Hills dacite (Tdw) coincide with both positive and negative magnetic anomalies. The main outcrop area of dacite (Tdw) in the eastern Wildcat Hills coincides with a positive magnetic anomaly (figures 4 and 5), which appears to continue beyond the outcrops to the east and forms a west-facing crescent around exposures of Oquirrh Formation (Pos) in the central part of the map. The high also extends westward beyond the dacite (Tdw) outcrops and under the easternmost outcrops of rhyolite (Qrw), reinforcing the stratigraphic relation (plate 2; A-A′) of the younger rhyolite (Qrw) overlying the older dacite (Tdw). Discontinuous exposures of dacite (Tdw) to the southeast and north of the Wildcat Hills (figures 1 and 7) coincide with magnetic lows that are present along the same west-facing arc as that defined by the magnetic highs, indicating that eruptions took place during both normal- and reversed-polarity chrons (see Geochronology section), but with similar structural control. It appears that the dacite (Tdw) erupted to form an arcuate series of domes and flows around the southeast, east, and northeast margins of the Oquirrh Formation (Pos), most of which are now buried by younger deposits. If this is correct, it means that the extent of the dacite (Tdw) is significantly greater than the area represented by the outcrops.

Although not found in the map area, the Hansel Valley ash is inferred to have erupted from somewhere near where Curlew Valley meets the northwest shore of Great Salt Lake (Miller and others, 1995, 2007). The basaltic tephra occurs as a distinctive dark brown bed that is generally less than 0.4 inch (1 cm) thick near the base of the Lake Bonneville lacustrine marl (Miller and others, 2007). It is chemically similar to the middle Pleistocene basalts in eastern Curlew Valley (figure 1), and grain size analyses also indicate the ash was erupted in that area and transported in an east-southeast direction to the Wasatch Front (Miller and others, 1995, 2007). The ash has an estimated age of about 26,500 ^{14}C yr B.P. based on radiocar-

bon ages for the marl (Oviatt and others, 1992), which makes it the youngest known volcanic unit to have erupted from the Curlew Valley area. It is present within Lake Bonneville marl northeast of Locomotive Springs and at Monument Point, but is absent in lower Deep Creek and points westward (figure 1). Oviatt and Miller (1997) traced the ash bed upslope from deepwater lake to shorezone facies, establishing that the ash was deposited in Lake Bonneville when the lake level was about 4380 feet (1335 m) altitude, and the lake was about 195 feet (60 m) deep (Miller and others, 2007). The eruptive center for the ash has not been discovered, presumably because the edifice was eroded by Lake Bonneville. A prominent, small-diameter negative anomaly in the aeromagnetic data south of Locomotive Springs Shield (figures 1 and 7) offered an intriguing possibility, but is the wrong polarity for the age of the unit, which corresponds to a normal polarity event.

QUATERNARY SURFICIAL DEPOSITS

Surficial deposits in the map area include Quaternary alluvial, eolian, and lacustrine sediments. Lacustrine sediments deposited during the rise and fall of Lake Bonneville, which was the youngest, deepest and most extensive pluvial lake in northern Utah (Oviatt and others, 1992; Godsey and others, 2005), are almost completely preserved. Coarse-grained deposits formed at wave-dominated shorelines are widespread around the Wildcat Hills and the shield volcanoes, and finer-grained, deeper-water deposits are widespread in the valleys. Lake Bonneville started rising about 30,000 years ago (30 cal ka; Oviatt and others, 1992; Oviatt, 2015) and left a prominent series of beach gravels at several lake levels, including several regionally recognized shorelines and/or shorezones. The earliest is the undated Pilot Valley shoreline of Miller and others (1990), which was the informal name given to transgressive shorezone gravel accumulations bordering Pilot Valley at 4285 feet (1306 m). In the southern part of the Kelton Pass SE quadrangle two southeast-facing gravel bars are preserved at about 4285 feet (1306 m) elevation (plate 1, Qlg), and are mapped as Pilot Valley shorezone deposits. The westernmost gravel bar was attributed to the Gilbert shoreline by Currey (1982, table 1B, point 40); however, the elevation of the beach crest is 25 feet (7 m) higher than the Gilbert shoreline. The two shorelines can be distinguished further on the basis of stratigraphy – the Pilot Valley shoreline is transgressive-phase, with marl overlying gravel, whereas the Gilbert shoreline is a high-stand that is characterized by gravel over marl. Currey (1982) erred by interpreting as the Gilbert the feature we identify as the Pilot Valley shoreline; correcting this error removes an anomalously high elevation Gilbert beach from his compilation.

The lake continued to rise until about 25 cal ka when the Stansbury oscillation occurred (Oviatt, 2015) and formed a prominent series of beach gravels from 4395 to 4550 feet (1340 to 1387 m) (Oviatt and others, 1990). These beach gravels (Qlg) are well preserved at numerous locations around the Wildcat Hills and the shield volcanoes. On Cedar Hill the uppermost Stansbury beach is at 4510 feet (1375 m), and the lacustrine gravel is mantled by marl and/or reworked marl (plate 1, Qlf/Qlg), evidence of transgressive-phase deposition. South of the Wildcat Hills a beach gravel complex occurs from 4360 to 4500 feet (1329 to 1372 m), and is attributed to the oscillation. The very lowest of these beaches is below the lower limit of 4395 feet (1340 m) established by Oviatt and others (1990), so it is either misattributed to the Stansbury oscillation, or could be evidence for a lower limit of the oscillation (the altitude of the lowest part of the oscillation is not known with certainty).

Following the Stansbury oscillation, the lake continued rising until about 18 cal ka when it reached its highest elevation (Oviatt, 2015). At this time, southern Curlew Valley and the area of both quadrangles were completely submerged, so the Bonneville shoreline is not present in the map area; however, it is well developed at about 5230 feet (1594 m) in Paleozoic rocks around Monument Peak (figure 1; Miller and Langrock, 1997a) and at about 5180 feet (1579 m) in alluvial fans on the east end of the Raft River Mountains (figure 1; Wells, 2009). Shortly after the lake reached its highest level, the overflow threshold near Zenda, Idaho, catastrophically failed and the lake receded to a stable lower threshold where it resided from about 18.1 to 15 cal ka (Godsey and others, 2005; Miller and others, 2013; Oviatt, 2015), creating the Provo shoreline. The Provo shoreline is expressed as a sharp wave-cut bench at 4810 to 4820 feet (1466 to 1469 m) in the rhyolite and dacite of the Wildcat Hills, and as a more subdued bedrock bench at the same elevation on Cedar Hill. A double barrier beach that is typical of Provo deposition (Miller and others, 2013) is present in gravel deposits (Qlg) that lie between the rhyolite (Qrw) and dacite (Tdw) (plate 1). Calcareous tufa deposits are common at the Provo shoreline.

Following the Provo stand, Lake Bonneville fell to levels possibly lower than average modern levels of Great Salt Lake (Curry, 1990; Oviatt and others, 1992), exposing a blanket of marl, sand, and gravel in eastern Curlew Valley. The Bonneville lake cycle ended about 13 cal ka (Oviatt, 2015), and was followed by a small transgression of the lake called the Gilbert episode, which peaked at about 11.6 cal ka (Oviatt, 2014). Features attributed to this transgression were compiled by Currey (1982) and designated the Gilbert shoreline. The features are both constructional and erosional, and range in elevation from 4242 to 4301 (1293 to 1311 m). Recent work by Oviatt (2014) has shown that the Gilbert-episode lake reached a maximum altitude of 4250 to 4255 feet (1295 to 1297 m), and suggests that many of the Gilbert shoreline features of Currey (1982), especially those higher than about 4255 feet (1295 m), were misidentified. Within the quadrangles, a subtle scarp near 4255 feet (1296 m) elevation is inferred to be a Gilbert-episode shorezone feature. The scarp is parallel to topgraphic contours, and oriented generally east-west, and is thus unlikely to be a fault. It is cut into alluvial and eolian

deposits that cover the Bonneville marl, indicating that if the scarp is lacustrine in origin, it postdates Lake Bonneville. A gently-sloping platform of well-sorted lacustrine sand that stretches southwest away from that scarp in the vicinity of Deep Creek, and overlies Bonneville marl, also could be related to the Gilbert episode. The Gilbert episode was followed by Great Salt Lake (Murchison, 1989; Oviatt and others, 2005; Oviatt, 2014), the level of which has fluctuated considerably. For most of historical time the average altitude has been near 4200 feet (1280 m). In the mid-1980s, however, it reached a high of 4212 (1284 m)—an elevation which brought it to within about one-quarter mile (400 m) of the southern boundary of the quadrangles.

Lake Bonneville profoundly modified and overprinted the landscape and geology within the map area. Subsequent erosion and alluvial and eolian deposition have modified that landscape only slightly, with the most notable feature being the entrenchment of Deep Creek and deposition along its floodplain, and alluvial fan deposition. The upper surface of the lacustrine marl that blanketed the area has been modified by wind and running water to produce a thin layer of reworked marl across most of the valley. Wind also reworked lacustrine sand into eolian dunes along the west side of the Wildcat Hills and near mudflats along the southern edge of the map area.

GEOLOGIC HAZARDS

Flooding and Gullying

Floods are possible in much of Curlew Valley. Debris flows and floods could occur on alluvial fans, and on broad alluvial terraces and plains near streams such as Deep Creek. The narrow canyon occupied by Deep Creek is a likely site for powerful flash floods. Flooding by Great Salt Lake also could occur. The mud flats in the Locomotive Springs and Monument Point quadrangles (figure 1) were flooded several times during the Holocene by rise of Great Salt Lake. Several of these floods were as extensive as the flood of the late 1980s (Atwood, 2006), when Great Salt Lake occupied beaches at Monument Point and flooded much of the marshland in Locomotive Springs Wildlife Management Area.

Gullying has occurred in many areas underlain by unconsolidated to moderately consolidated sediments. The fine-grained Quaternary deposits are highly susceptible to the erosion that results from the destruction of natural ground cover.

Earthquake Hazards

Northern Utah is part of a seismic belt characterized by numerous small-magnitude seismic events and by potential for infrequent major events (Smith and Sbar, 1974; Christenson and others, 1987). Historical felt earthquakes include two magnitude (M) 6 events in Hansel Valley (east of the Hansel Mountains; figure 1)—one in 1909 (M 6, estimated) and one in 1934 (M 6.6) (Walter, 1934; Arabasz and McKee, 1979; Doser, 1989). Frequent smaller-magnitude earthquakes (M<4) occur in a broader area that includes Curlew and Hansel Valleys, northern Great Salt Lake, and the Rozel Hills located south of figure 1 (Christenson and others, 1987; Hecker, 1993). Current resources pertaining to earthquake activity in Utah are provided online by the University of Utah at http://quake.utah.edu/index.shtml, the UGS at http://geology.utah.gov/hazards/earthquakes-faults/utah-earthquakes-2/, and the USGS at http://earthquake.usgs.gov/earthquakes/.

Quaternary faults in Hansel Valley include those mapped in the Monument Point and Monument Peak quadrangles and subparallel faults about one mile (1.6 km) to the east (figure 1) that were studied by Robison and McCalpin (1987) and McCalpin and others (1992). Quaternary faults are also inferred by several workers to lie within the northwestern part of Great Salt Lake (Hecker, 1993; Dinter and Pechmann, 2014). The inferred Coyote Spring fault may cut Pleistocene basalt in the west part of the Monument Peak NW quadrangle (figure 1). Vegetation lineaments visible in aerial photography are present in the map area (plate 1) and surrounding Curlew Valley, and may in part be faults of Holocene age. These faults and lineaments may suggest a Quaternary record of surface rupture due to seismic events.

The 1934 magnitude 6.6 earthquake in Hansel Valley (Christenson and others, 1987) produced surface rupture along four cracks (Adams, 1938), some of which show evidence for earlier displacements (Robison and McCalpin, 1987; McCalpin and others, 1992). The earthquake caused severe damage in local towns and ranches, and it even caused damage in cities along the Wasatch Front. The occurrence of historical earthquakes in this area signifies that the threat of future earthquakes is real. The recurrence interval of large, surface-faulting earthquakes appears to be several thousand years (McCalpin and others, 1992), but the pattern of recurrence is complex and not easily converted as a predictive tool.

The regional history of seismic activity (Christenson and others, 1987; Hecker, 1993) and evidence for Quaternary faults in Curlew and Hansel Valleys raises the possibility of moderate to large local earthquakes. If even a small number of the lineaments in the map area (plate 1) and surrounding Curlew Valley (Miller, 1997a, 1997b, 1997c; Miller and Langrock, 1997a) represent Holocene fault ruptures, the potential for M>6 earthquakes in Curlew Valley is greater than has been previously estimated. The active Wasatch fault zone and related faults 45 miles (70 km) to the east (Smith and Bruhn, 1984; Hecker, 1993) present a potential for a major seismic event that also could strongly shake the Curlew Valley area. In addition to ground shaking and surface rupture, earthquake hazards in this region include lateral spreads, liquefaction, rockfalls, and debris flows.

Volcanic Hazards

The youthful ages of Quaternary volcanic units and associated eruptive centers in eastern Curlew Valley, the youngest of which could be the unidentified source of the ~26,500 ^{14}C yr B.P. Hansel Valley basaltic ash (Miller and others, 2007) found in the vicinity of Great Salt Lake, suggest a possibility for future eruptions. Although most eruptions produced basaltic lava flows, which is a hazard relatively easy to mitigate in sparsely populated areas, the presence of basaltic ash indicates that explosive eruptions also took place. Future eruptions could potentially take place within Great Salt Lake or adjacent marshes, potentially producing an explosive hydromagmatic eruption. Even a small explosive eruption would heavily impact local ranches and communities and, given the distribution of the Hansel Valley ash south and east of Curlew Valley (Miller and others, 2007), also could impact the people and infrastructure of the Wasatch Front. Modern seismicity is most prevalent in the Hansel Mountains and Valley (figure 1); however, numerous epicenters (data available from the Utah Automated Geographic Data Center at ftp://ftp.agrc.utah.gov/UtahSGID_Vector/UTM12_NAD83/GEOSCIENCE/PackagedData/_Statewide/SeismologyVolcanology/) are near the Quaternary basalts (Qb) in Curlew Valley, strengthening the suggestion that volcanic activity is part of the modern tectonics of the area.

ECONOMIC GEOLOGY

Water

There are no springs or perennial streams within the map area. Approximately 30 water wells have been drilled in low-lying parts of the map area for agricultural purposes. A comprehensive study of the geology and chemistry of the Curlew Valley groundwater system was conducted by Hurlow and Burk (2008) to investigate the decrease in groundwater levels and degradation in water quality that has occurred during the past 30 years, in part due to increased agricultural use. The groundwater system is characterized as a basin-fill aquifer that is recharged mainly from infiltration of snow-melt and runoff from adjacent mountain ranges (Hurlow and Burk, 2008). The horst (described previously) that extends between the Wildcat Hills and Curlew Junction (figure 1) forms a bedrock divide between the Kelton flow system to the west, and the combined flow of the Juniper-Black Pine and Holbrook-Snowville systems to the east. Regional groundwater flow is south toward Great Salt Lake (Hurlow and Burk, 2008).

Sand and Gravel

Lacustrine sand and gravel deposits of Lake Bonneville form thick platforms surrounding most bedrock exposures, some of which may be suitable for use in road construction and as fill for local construction. The largest accumulations of gravel are indicated on the map (plate 1) as lacustrine gravel (Qlg). Eolian sand deposits generally contain mud pellets, gypsum, and ooids, making them unsuitable for many construction purposes. No sand and gravel quarries were observed in the map area.

Minerals

A source for silica may be found in the sandstone member of the Oquirrh Formation (Pos). Rock in this member commonly is highly fractured and silicified, possibly making it of value as an easily mined, but somewhat impure, silica source. It also could serve as a potential source for road metal.

Perlite (volcanic glass with a higher water content than obsidian) is prevalent in the Wildcat Hills rhyolite (Qrw). It is commonly used in horticulture as a soil amendment; in construction materials such as plasters, insulation and ceiling tiles; and as a filtration aid. No mineral prospects were observed in the area mapped.

Energy

Hydrocarbon exploration was conducted by the Stanford Petroleum Company just south of the Wildcat Hills (plate 1, SP) where a test hole was drilled to a depth of 679 feet (207 m), supposedly bottoming in Pennsylvanian strata. The hole was drilled and abandoned in 1946. From 1954 to 1956 Utah Southern Oil Company drilled several test holes in the Monument Peak NW quadrangle (figure 1) to depths between 4765 to 7569 feet (1452 to 2307 m). All of the holes bottomed in Paleozoic sedimentary strata. Only minor shows of gas were encountered (Peace, 1956), and the wells were subsequently abandoned.

The presence of Pleistocene volcanic units, warm water discharging from Coyote Spring (figure 1), and proximity to the Raft River geothermal area to the north in Idaho, suggest that southern Curlew Valley may have potential as a low-temperature geothermal resource. The geothermal potential of the area has been studied (Davis, 1984; and Davis and Kolenar, 1984), and thus far has not been considered viable for development. Blackett and Wakefield (2002) compiled a digital atlas of geothermal resources for the state of Utah, and Young and others (2013) studied the geothermometry of thermal springs in northern Utah (including Coyote Spring) and southeastern Idaho in an attempt to determine the temperature of the associated hydrothermal reservoir. Current information pertaining to geothermal resources in Utah, including a comprehensive bibliography and reference list, is provided online by the UGS at http://geology.utah.gov/resources/energy/geothermal/.

GEOLOGIC UNIT DESCRIPTIONS

QUATERNARY SURFICIAL DEPOSITS

Alluvial Deposits

Qal **Alluvium** (Holocene) – Poorly sorted sand, silt, and clay in ephemeral stream channels; locally includes minor gravel; most extensive mapped deposits are in Deep Creek channel; many other channels contain deposits too narrow to depict on map; thickness variable, generally less than 20 feet (6 m).

Qafy **Younger alluvial-fan deposits** (Holocene) – Poorly sorted gravel, sand, silt, and clay forming small alluvial fans, mostly around the flanks of the Wildcat Hills and along the west side of Curlew Valley; unit postdates deposits of Lake Bonneville; thickness variable, generally less than 30 feet (10 m).

Qam **Alluvial mud** (Holocene) – Pale brown clay and silt underlying mudflats along southern map border and bordering Great Salt Lake; commonly sticky, soft, and damp; south of the Old Central Pacific Railroad Grade, below about 4220 feet (1286 m), includes lacustrine mud from Holocene highstands of Great Salt Lake, which is similar in appearance; thickness variable, generally less than 30 feet (10 m).

Eolian Deposits

Qed **Eolian sand dunes** (Holocene) – Dunes of fine to medium sand; adjacent to streams and eroded edges of mudflats; forms linear patterns decorating topographic breaks; most prominent along west side of Wildcat Hills and near the mudflats along southern edge of map area; thickness variable, generally less than 7 feet (2 m).

Lacustrine Deposits

Qlf **Lacustrine fine-grained deposits** (upper Pleistocene) – White, pale brown, and tan silt, clay, and fine-grained sand deposited by Lake Bonneville; laminated to thin bedded; mapped south of Wildcat Hills in a low area behind a Qlg gravel bar complex; represents environments where rate of terrigenous influx overwhelmed rate of marl deposition; also mapped where marl was reworked into thin mantle of silty sheetwash deposits; thickness uncertain, but probably less than 20 feet (6 m).

Qlm **Lacustrine marl** (upper Pleistocene) – White, pink, and pale-brown marl deposited by Lake Bonneville; contains abundant ostracodes and sparse dropstones; lower part typically white and laminated; upper part pink to pale brown and less distinctly bedded; locally includes sand beds and gravel lenses; south of Wildcat Hills, and below Gilbert shoreline, includes a thin, overlying unit of latest Pleistocene to Holocene(?) pale brown, calcareous mud and ooid sand; thickness from about 3 to 15 feet (1 to 5 m).

Qls **Lacustrine sand** (upper Pleistocene) – Pale brown, well-sorted, fine- to medium-grained sand deposited by Lake Bonneville; composed almost entirely of sand derived from rhyolite in areas adjacent to outcrops of Qrw; thick deposits occur below the Provo shoreline in and along the east side of the Wildcat Hills, and at the base of the north side of Middle Shield (figure 1); extensive thin deposits are present on both sides of Deep Creek, below the Gilbert shoreline; thickness less than about 50 feet (15 m).

Qlg **Lacustrine gravel** (upper Pleistocene) – Cobble and pebble gravel, moderately well sorted with sand, silt, or tufa matrix; forms spits and barrier bars, and mantles steep slopes adjacent to bedrock outcrops; most mapped deposits are associated with the Stansbury oscillation of Lake Bonneville; lesser accumulations present at the Pilot Valley and Provo shorelines; a Stansbury beach complex lies south of the Wildcat Hills dacite (Tdw) between 4360 and 4500 feet (1329 and 1372 m) and consists of 11 beach-gravel accumulations and many more minor accumulations; a Stansbury gravel spit and broad barrier beach are well preserved on the west side of Wildcat Hills between 4485 and 4500 feet (1367 and 1372 m); deposits are present on both shield volcanoes within the elevation range of the Stansbury oscillation; thickness less than about 50 feet (15 m).

Qlgs **Lacustrine gravel and sand** (upper Pleistocene) – Moderately- to well-sorted gravel and sand deposited by Lake Bonneville; accumulated in nearshore settings, adjacent to bedrock outcrops along the southwest side of Wildcat Hills, and southeast part of Middle Shield; forms deposits similar to the gravel (Qlg) beaches, but differs from them by containing a high proportion of sand; unit probably represents deposition in lower energy environment than that of gravel beaches; thickness less than about 50 feet (15 m).

Mixed-Environment Deposits

Qae **Mixed alluvial and eolian deposits** (Holocene) – Pale-brown fine-grained deposits of mixed origin, generally complexly intermixed and not mappable as distinct units; commonly displays small dunes and mounds; generally found in low-lying nearly flat areas, including most of western Curlew Valley; thickness uncertain, but probably less than 20 feet (6 m).

Qla **Lacustrine and alluvial deposits, undivided** (Holocene and upper Pleistocene) – Complexly mixed lacustrine and alluvial deposits, in most places consisting of thin alluvium overlying and interbedded with lacustrine deposits; located between Bonneville shoreline and Gilbert shorezone; thickness uncertain, but probably less than 20 feet (6 m).

Stacked-Unit Deposits

The following stacked units describe areas where Lake Bonneville deposits form a thin veneer over bedrock and other lacustrine units. The unit labels are shown on the map separated by a slash (/), with the younger, overlying unit listed first.

Qlf/Qlg **Lacustrine fine-grained deposits over lacustrine gravel** (upper Pleistocene over upper Pleistocene) – Marl deposited during a regressive phase of Lake Bonneville and subsequently reworked, overlying gravel deposits from an an earlier, transgressive phase of the lake; mapped along west side of Cedar Hill; thickness of upper unit is less than 3 feet (1 m).

Qlg/unit (Qlg/Tb?, Qlg/Pos)

Lacustrine gravel over unit (upper Pleistocene over Tertiary through Permian) – Lacustrine gravel overlying possible Tertiary basaltic lava flows (Tb) and Oquirrh Formation (Pos) south of Wildcat Hills; thickness of upper unit is less than 15 feet (5 m).

Qlgs/Ts **Lacustrine gravel and sand over Salt Lake Formation** (upper Pleistocene over Tertiary) – Lacustrine gravel and sand overlying tuffaceous sedimentary rocks of the Salt Lake Formation (Ts) at south end of Wildcat Hills; thickness of upper unit is less than 15 feet (5 m).

QUATERNARY AND TERTIARY VOLCANIC ROCKS

Rock names for volcanic units were derived by plotting geochemical data from Shea (1985), Kerr (1987), Miller and others (1995), and unpublished sources (table 4) on the total alkali-silica classification diagram of LeBas and others (1986; figure 14). Units younger than 2.58 Ma are assigned a Quaternary age based on the recent ratification of a proposal by the International Commission on Stratigraphy to lower the base of the Quaternary System and the Pleistocene Series from 1.81 to 2.58 Ma (Gibbard and others, 2009).

Qb **Basalt** (Pleistocene) – Medium-gray to medium-dark-gray, weathering to moderate-brown, dense to very vesicular basalt; generally microporphyritic, with phenocrysts (10 to 15%) of plagioclase, olivine, and pyroxene in aphanitic groundmass; detailed studies of the petrography and petrology of these flows were conducted by Shea (1985), Kerr (1987), and Miller and others (1995); individual lava flows are generally less than about 10 feet (3 m) thick and weather to low ledges; primary flow features such as glassy pahoehoe surfaces and levees are locally well preserved; forms two shield volcanoes east of Deep Creek; Cedar Hill, located in northeast corner of map area and adjacent Monument Peak quadrangle to east, is about 4 miles (6 km) in diameter, and 700 feet (213 m) high; informally named Middle Shield in southeast corner of map area is 3 miles (5 km) in diameter, and 400 feet (122 m) high; both shields have summit craters partly filled with lacustrine sediments; lava erupted primarily from summit craters and traveled as sheets or long, narrow tongue-shaped flows down volcano flanks; flows with well-preserved primary morphology on south and east sides of both shields probably represent youngest flows erupted from these volcanoes; queried where outlying non-contiguous basalt outcrops are inferred to be remnants of lava flows from these volcanoes on basis of proximity; Miller and others (1995) reported K-Ar whole-rock ages of 1.16 ± 0.08 Ma from flow on summit of Cedar Hill (sample M89CV-43, Monument Peak quadrangle, figure 1), and 0.72 ± 0.15 Ma from a distal flow from Middle Shield (sample M89CV-4, Locomotive Spring quadrangle, figure 1); outcrops coincide with prominent aeromagnetic highs (figures 4, 5 and 7), indicating the volcanoes erupted during a normal polarity chron; exposed thickness about 700 feet (213 m).

Qrw **Rhyolite of Wildcat Hills** (Pleistocene) – Gray and grayish-pink to black, porphyritic, flow-foliated, high-silica rhyolite lava flows and/or domes; phenocrysts (1-10%) of rounded quartz, euhedral to subhedral sanidine and plagioclase, and euhedral biotite; quartz, sanidine, and plagioclase account for about 99% of the phenocrysts, and are present in approximately equal amounts; groundmass varies from glassy to finely crystalline; forms cliffs, ledges, and knobby outcrops; detailed studies of the petrography and petrology of these flows were conducted by Howes (1972), Shea (1985), and Miller and others (1995); locally contains xenoliths of basalt (Tb), Salt Lake Formation (Ts), and Oquirrh Formation (Pos) from 0.4 to 6 inches (1 to 15 cm) in longest diameter; devitrification and hydration textures are prevalent and include spherulites and lithophysae that range in size from about 0.1 to 16 inches (0.25 to 40 cm), and perlite; textural facies typical of subaerial silicic lava flows (Christiansen and Lipman,1966; Fink, 1983; McPhie and others, 1993; Duffield and others, 1995) are present throughout unit as discontinuous zones, or eroded outcrops too small to map;

facies include black vitrophyre/obsidian, gray, finely to coarsely pumiceous lava, and reddish-brown to grayish-orange-pink carapace breccia, which Howes (1972) referred to as a welded tuff; forms western Wildcat Hills, with northwest-elongate exposures approximately 3.5 miles (5.6 km) long by 2.3 miles (3.8 km) wide, and 5.4 square miles (14.1 km^2); near-vertical ribs of perlitic, spherulitic, and lithophysae-rich rhyolite with foliation that strikes generally parallel to outcrop edge, occur along margins of rhyolite body; interpreted by Howes (1972) and Shea (1985) as dikes that intruded extensional fractures formed in the hinge of a trapdoor caldera but herein reinterpreted to be pressure ridges that formed during flow emplacement; base is not exposed, but unit is inferred to rest unconformably on tilted Salt Lake Formation (Ts) and probably Tertiary basaltic lava flows (Tb); sample F06_306CV yielded an $^{40}Ar/^{39}Ar$ sanidine age of 2.331 ± 0.010 Ma, slightly older than the K-Ar sanidine age of 2.1 ± 0.1 Ma reported by Miller and others (1995) for sample M93WI-40; outcrops of this unit coincide with magnetic lows (figures 4 and 5), consistent with the $^{40}Ar/^{39}Ar$ age, which is entirely within a reversed polarity chron; estimated volume is about 0.2 cubic miles (0.8 km^3), and thickness is about 200 feet (60 m).

Tdw **Dacite of Wildcat Hills** (Pliocene) – Medium-dark-gray and pale-red-purple, weathering to dark-gray and grayish-red, high-silica dacite lava flows with phenocrysts (about 10 to 20%) of plagioclase, pyroxene and quartz, and xenocrysts (5 to 10%) of sieve-textured plagioclase; plagioclase xenocrysts, which are the most conspicuous macroscopic feature, are angular, reach about 1 inch (2.5 cm) in size, and are easily misidentified as xenoliths; phenocrysts of pyroxene (5%), plagioclase (1 to 5%), and quartz (1%) are subhedral to anhedral, and generally less than 0.1 inch (3 mm) in diameter; groundmass typically dense, and variably devitrified; calcite alteration is prevalent; locally contains basalt (Tb) and Salt Lake Formation xenoliths to 4 inches (10 cm) in diameter; weathers to low-relief cliffs, ledges, and rounded, knobby outcrops; commonly flow-banded, with near-vertical joints that may represent incipient columnar jointing or other cooling features; vitrophyre and flow breccia are present locally, and probably represent the base and top of individual flows; flow breccia is variegated orange and black, 1 to 7 feet (0.3 to 2 m) thick, and interfingers with or overlies flow-banded dacite; contact between breccia and adjacent flow-banded lava is typically irregular, with textures comingling, and sparse spherulites, lithophysae, and vesicles present in the flow-banded rocks; Howes (1972) interpreted the flow breccia as diatremes, and Shea (1985) as a welded ash flow tuff that was compositionally indistinguishable from the dacite lava; largest dacite body forms eastern Wildcat Hills and occupies an area of approximately 2.3 square miles (6 km^2); smaller, non-contiguous outcrops are present to the southeast of the main body, and to the northwest outside the map area (figure 1); flow foliation data suggest that the dacite may have been emplaced as a series of thick flows erupted from multiple vents, with the main eruptive center underlying eastern Wildcat Hills, and the non-contiguous outcrops representing other vent areas; the vent location derived from the foliation data for the main dacite body coincides with a prominent north-northeast-trending valley that bisects the dacite; base of dacite is not exposed, but based on nearby outcrops it could unconformably overlie some combination of Oquirrh Formation (Pos), Salt Lake Formation (Ts), or Tertiary basaltic lavas (Tb); U-Pb zircon data from sample F06_371CV indicate unit is 2.8 ± 0.03 Ma (figure 9; table 2), which is significantly younger than the K-Ar plagioclase age of 4.4 ± 1.1 Ma reported by Miller and others (1995) for sample M93WI-37 (table 1); outcrops coincide with positive and negative magnetic anomalies (figures 4 and 5) indicating eruptions spanned multiple polarity chrons; exposed thickness about 200 to 300 feet (60 to 90 m).

Tb **Basaltic lava flows** (Pliocene) – Dark gray, weathering to moderate brown, vesicular basalt; generally microporphyritic, with phenocrysts (10 to 20%) of plagioclase and olivine in a groundmass of plagioclase, augite, olivine, and oxides; locally includes abundant xenoliths of Salt Lake Formation (Ts) and Permian quartzite (Pos) to 8 inches (20 cm), and quartz inclusions to 0.6 inch (1.5 cm); detailed studies of the petrography and petrology of these flows were conducted by Howes (1972), Shea (1985), and Kerr (1987); exposed south and southwest of Wildcat Hills as isolated, eroded, and partially buried remnants of flows and possibly shallow intrusions or dikes; northernmost outcrop area includes scoria, suggesting proximity to vent, and about 0.25 mile (0.4 km) to south, a small, circular, columnar-jointed outcrop has well-developed, near-vertical columns 8 to 20 inches (20 to 50 cm) in diameter, and is inferred to be a neck; southernmost outcrop in map area, which is chemically a tephrite or basanite (figure 10, table 4), also has well-developed, vertical columns that are 3 to 5 feet (1-2 m) in diameter and at least 13 feet (4 m) high; base is poorly exposed in outcrops closest to Wildcat Hills, where a flow appears to conformably overlie bedded scoria, which in turn overlies tuffaceous diamictite of Salt Lake Formation (Ts) on a possible angular unconformity; outcrops of Wildcat Hills rhyolite (Qrw) just upslope are inferred to overlie basalt, although contact is not exposed; queried where existence inferred from abundant float; K-Ar whole rock ages of 3.6 ± 0.1

Ma (sample M93WI-43) and 4.9 ± 0.4 Ma (sample AD/WH/91-7) reported by Miller and others (1995) (table 1); outcrops coincide with very subtle positive and negative magnetic anomalies (<1-2 nT) indicating eruptions spanned multiple polarity chrons; exposed thickness about 200 feet (60 m).

TERTIARY SEDIMENTARY ROCKS

Ts **Salt Lake Formation, undivided** (Miocene) – White and very light gray to yellowish-gray and very pale orange, tuffaceous sedimentary rocks, conglomerate, and vitric air fall tuff; thin- to medium-bedded and complexly interlayered; thin silica veins and zeolite alteration present locally; outcrops are poorly to moderately indurated, and weather to soft, light-colored slopes around south end of Wildcat Hills, typically mantled by Pleistocene lacustrine sediments; bedding is tilted and folded in a wide range of attitudes; locally includes planar parallel surfaces that either mark bedding planes or are tectonic fractures (plate 1, planar feature of uncertain origin); lower contact is not exposed, but unit is inferred to overlie Oquirrh Formation (Pos) based on field relations; unconformably overlain and intruded by Tertiary basaltic lavas (Tb), and inferred to be overlain by rhyolite (Qrw) based on field relations; thickness is poorly constrained due to lack of exposed base and structural complexity, but one area of near-vertical beds measures about 600 feet (180 m) in thickness; gravity data suggest thickness could be up to 5000 feet (760 m); main lithofacies are described, but not mapped separately:

Tuffaceous sedimentary rocks – Tuffaceous sandstone and limestone make up bulk of section; sandstone is poorly sorted, very fine to coarse grained, commonly calcareous; interbedded with thin, platy beds of resistant limestone; limestone is locally fossiliferous, and includes sparse gastropods tentatively identified as Neogene freshwater forms such as *Menetus* and *Planorbula*, and small, poorly preserved bivalves that could not be identified (D. Elliot, Northern Arizona University, written communication, July 2010); locally contains siltstone, tuffaceous siltstone, and lignite.

Conglomerate – Yellowish gray or very pale orange, clast-supported with poorly-sorted, subangular to subrounded pebble to boulder-size clasts of Paleozoic sedimentary rocks in a non-calcareous coarse sand matrix; crudely bedded; east of main Tertiary basalt outcrop (Tb), clasts are almost exclusively quartzite derived from adjacent outcrops of brecciated sandstone and quartzite of the Oquirrh Formation (Pos); west of basalt (Tb), clast assemblage is heterolithologic and includes mostly Oquirrh Formation quartzite, lesser amounts of Paleozoic limestone, and minor dark chert; beds of distinctive clast-supported, chert-pebble conglomerate present locally, and consist of moderately- to well-sorted, subangular to subrounded chert pebbles and sparse clasts of pertrified wood.

Vitric air fall tuff – Gray, generally massive, fine- to medium-grained with visible bubble-wall glass shards; tephrochronological analysis of sample wch09-1483 yielded no firm correlation, but composition is generally similar to tephra erupted from the Twin Falls volcanic field along the Yellowstone hotspot track, which erupted multiple times between about 10.5 and 8.5 Ma (M. Perkins, University of Utah, written communication, May 18, 2010); to west unit Ts ranges from about 6 to 16 Ma (Perkins, 2014).

PERMIAN AND PENNSYLVANIAN SEDIMENTARY ROCKS

Stratigraphic nomenclature for the Permian-Pennsylvanian Oquirrh Formation in northwestern Utah is poorly established and varies by author. A compilation of the geology of Curlew Valley, northwestern Utah and south-central Idaho by Hurlow and Burk (2008) attempted to address this variability, and condensed seven different nomenclatures into a two-fold scheme. This included a reinterpretation of the nomenclature used by Miller (1997a-c) and Miller and Langrock (1997a-c), based partly on limited biostratigraphic data. It is unclear how applicable the nomenclature is to strata of the northern Oquirrh sub-basin as a whole. For this reason, this map retains the Oquirrh Formation nomenclature originally used by Miller and Langrock (1997b) for the interim geologic map of the Monument Peak SW quadrangle.

Pos **Oquirrh Formation, sandstone member** (Lower Permian) – Light-gray, weathering yellowish-gray to brown, well-indurated, well-sorted quartz sandstone and orthoquartzite; overall grain size varies from very fine to medium; occurs as ledge- and cliff-forming outcrops south of Wildcat Hills; locally calcareous and fusulinid-bearing; unit is massive and highly fractured, making identification of bedding nearly impossible and suggesting unit underwent substantial structural deformation; planar parallel surfaces that either mark bedding planes or are tectonic fractures, are prevalent throughout the outcrops, and are mapped as ”planar feature of uncertain origin” (plate 1); basal and upper contacts are not exposed; contact with overlying Salt Lake Formation (Ts) inferred to be an erosional unconformity marked locally by thin, reddish, poorly sorted sediments inferred to represent a paleosurface (Paleosol location, plate 1); fusulinid fossil taxa found in sample F09_154CV include poor-

ly preserved (highly abraded, possibly reworked?) *Schwagerina* and *Triticites* cf. *T. cellamagnus*, which have an age of early Wolfcampian (Early Permian) (A.J. Wells, independent paleontologist, written communication to Utah Geological Survey, 2009); thickness of the sandstone unit is poorly constrained due to lack of contacts and bedding, and structural complications, but exposed thickness is estimated to be about 300 to 400 feet (90 to 120 m); Miller and Langrock (1997a) reported a thickness of greater than 9500 feet (2900 m) for the same unit in the Monument Point quadrangle to the east (figure 1).

PIPo Oquirrh Formation, undivided (Lower Permian to Lower Pennsylvanian) – Shown on cross section only. Peace (1956) reported about 3000 feet (1000 m) of total Oquirrh Formation in the Federal No. 1 well in the Monument Peak NW quadrangle, and Wells (2009) reported 4000 feet (1200 m) of total Oquirrh Group in the Kelton Pass quadrangle.

ACKNOWLEDGMENTS

This project benefited substantially from the time and effort of numerous people. Jack Oviatt, Kansas State University (KSU) generously spent time with us in the field, providing insight into the Lake Bonneville history. David Elliot (Northern Arizona University) provided identification of fossils in the Salt Lake Formation, and A.J. Wells (independent, Exxon retired) identified fusulinids in the Oquirrh Formation. Mike Perkins (University of Utah) provided tephrochronology analysis of Salt Lake Formation tuff. Holly Langrock assisted in the field, and Don Clark (UGS) provided logistical support that facilitated the project work. Delbert Olsen and other residents of Snowville, Utah, provided hospitality, knowledge of the area, and interest in the project. Conversations with Eric Christiansen (Brigham Young University) and Geoff Phelps (USGS), informal reviews by Sue Beard (USGS) and Wendell Duffield (USGS, retired), and formal reviews by Ernie Anderson (USGS), Jack Oviatt (KSU), and Don Clark, Jon King, Grant Willis, and Michael Hylland (all UGS) greatly improved the final report. UGS staff prepared the final cartography, GIS data, and figures.

REFERENCES

Adams, T.C., 1938, Land subsidence north of Great Salt Lake, Utah: Bulletin of the Seismological Society of America, v. 28, p. 65–70.

Arabasz, W.J. and McKee, M.E., 1979, Utah earthquake catalog 1850–June 1962, *in* Arabaz, W.J., Smith, R.B., and Richins, W.D., editors, Earthquake Studies in Utah 1850–1978: Department of Geology and Geophysics, University of Utah, p. 1–14.

Atwood, G., 2006, Shoreline superelevation—evidence of coastal processes of Great Salt Lake, Utah: Utah Geological Survey Miscellaneous Publication 06–9, 231 p.

Baker, C.H., 1974, Water resources of the Curlew drainage basin, Utah and Idaho: Utah Department of Natural Resources, Division of Water Rights Technical Publication No. 45, 61 p.

Baranov, V.I., 1957, A new method for interpretation of aeromagnetic maps—pseudo-gravimetric anomalies: Geophysics, v. 22, p. 359–383.

Blackett, R.E., and Wakefield, S., 2002, Geothermal resources of Utah—a digital atlas of Utah's geothermal resources: Utah Geological Survey Open-File Report 397, CD-ROM.

Blakely, R.J., and Simpson, R.W., 1986, Approximating edges of source bodies from magnetic or gravity anomalies: Geophysics, v. 51, p. 1,494–1,498.

Cande, S.C., and Kent, D.V., 1995, Revised calibration of the geomagnetic polarity timescale for the Late Cretaceous and Cenozoic: Journal of Geophysical Research, v. 100, p. 6,093–6,095.

Channell, J.E.T., Mazaud, A., Sullivan, P., Turner, S., and Raymo, M.E., 2002, Geomagnetic excursions and paleointensities in the Matuyama Chron at Ocean Drilling Program Sites 983 and 984 (Iceland Basin): Journal of Geophysical Research, v. 107, no. B6, p. EPM 1-1–EPM 1-14.

Christenson, G.E., Harty, K.M., and Hecker, S., 1987, Quaternary faults and seismic hazards, western Utah, *in*, Kopp, R.S. and Cohenour, R.E., editors, Cenozoic geology of western Utah: Utah Geological Association Publication 16, p. 389–400.

Christiansen, R.L. and Lipman, P.W., 1966, Emplacement and thermal history of a rhyolite lava flow near Fortymile Canyon, southern Nevada: Geological Society of America Bulletin, v. 77, p. 671–684.

Cook, K.L., Halverson, M.D., Stepp, J.C., and Berg, J.W., Jr., 1964, Regional gravity survey of the northern Great Salt Lake Desert and adjacent areas in Utah, Nevada, and Idaho: Geological Society of America Bulletin, v. 75, p. 715–740.

Cordell, L., and Grauch, V.J.S., 1985, Mapping basement magnetization zones from aeromagnetic data in the San Juan Basin, New Mexico, *in* Hinze, W.J., editor, The utility of regional gravity and magnetic anomaly maps: Tulsa, Society of Exploration Geophysicists, p. 181–192.

Covington, H.R., 1983, Structural evolution of the Raft River basin, Idaho, *in* Miller, D.M., Todd, V.R., and Howard, K.A., editors, Tectonic and stratigraphic studies in the eastern Great Basin: Geological Society of America Memoir 157, p. 229–237.

Currey, D.R., 1982, Lake Bonneville—selected features of relevance to neotectonic analysis: U.S. Geological Survey Open-File Report 82-1070, 30 p.

Currey, D.R., 1990, Quaternary paleolakes in the evolution of semidesert basins, with special emphasis on Lake Bonneville and the Great Basin, U.S.A.: Palaeogeography, Palaeoclimatology, Palaeoecology, v. 76, p. 189–214.

Davis, M.C., 1984, Evaluation of low-temperature geothermal potential in north-central Box Elder County, Utah: Logan, Utah State University, M.S. thesis, 130 p., 7 plates.

Davis, M.C., and Kolenar, P.T., 1984, Low-temperature geothermal energy potential, north-central Box Elder County, Utah: Utah Geological and Mineralogical Survey Open-File Report 47, 112 p.

Dinter, D.A., and Pechmann, J.C., 2014, Paleoseismology of the Promontory segment, East Great Salt Lake fault: University of Utah, Final Technical Report submitted to the U.S. Geological Survey, National Earthquake Hazards Reduction Program, award no. 02HQGR0105, 23 p.

Doelling, H.H., 1980, Geology and mineral resources of Box Elder County, Utah: Utah Geological and Mineral Survey Bulletin 115, 251 p., 3 plates, scale 1:125,000, with contributions by J.A. Campbell, J.W. Gwynn, and L.I. Perry.

Doser, D.I., 1989, Extensional tectonics in northern Utah–southern Idaho, U.S.A., and the 1934 Hansel Valley sequence: Physics of the Earth and Planetary Interiors, v. 54, p. 120–134.

Duffield, W.A., Richter, D.H., and Priest, S.S., 1995, Geologic map of the Taylor Creek rhyolite and adjacent rocks, Catron and Sierra Counties, New Mexico: U.S. Geological Survey Miscellaneous Investigations Series Map I-2399, 16 p., 1 plate, scale 1:50,000.

Felger, T.J., Miller, D.M., Langenheim, V.E., Fleck, R.J., Perkins, M.E., and Wells, M.L., 2011, Structural and volcanic evolution of southern Curlew Valley, northwest Utah: Geological Society of America Abstracts with Programs, v. 43, no. 4, p. 49.

Fink, J.H., 1983, Structure and emplacement of a rhyolitic obsidian flow—Little Glass Mountain, Medicine Lake Highland, northern California: Geological Society of America Bulletin, v. 94, p. 362–380.

Fleck, R.J., Sutter, J.F., and Elliot, D.H., 1977, Interpretation of discordant $^{40}Ar/^{39}Ar$ age-spectra of Mesozoic tholeiites from Antarctica: Geochimica et Cosmochimica Acta, v. 41, p. 15–32.

Geodata International, Inc., 1979, Aerial gamma ray and magnetic survey, Brigham City national topographic map, Utah and Idaho: U.S. Department of Energy Report GJBX-124(79), scale 1:500,000.

Gibbard, P.L., Head, M.J., Walker, M.J.C., and the Subcommission on Quaternary Stratigraphy, 2009, Formal ratification of the Quaternary System/Period and the Pleistocene Series/Epoch with a base at 2.58 Ma: Journal of Quaternary Science, v. 25, p. 96–102.

Godsey, H.S., Currey, D.R., Chan, M.A., 2005, New evidence for an extended occupation of the Provo shoreline and implications for regional climate change, Lake Bonneville, Utah, USA: Quaternary Research, v. 63, p. 212–223.

Grauch, V.J.S., and Cordell, L., 1987, Limitations of determining density or magnetic boundaries from the horizontal gradient of gravity or pseudogravity data: Geophysics, v. 52, no. 1, p. 118–121.

Hecker, S., 1993, Quaternary tectonics of Utah with emphasis on earthquake-hazard characterization: Utah Geological Survey Bulletin 127, 157 p.

Howes, R.C., 1972, Geology of the Wildcat Hills, Utah: Logan, Utah State University, M.S. thesis, 50 p., 2 plates, scale 1:12,000.

Hurlow, H.A. and Burk, N., 2008, Geology and ground-water chemistry, Curlew Valley, northwestern Utah and south-central Idaho—implications for hydrogeology: Utah Geological Survey Special Study 126, 185 p., 2 plates.

Janoušek, V., Farrow, C.M., and Erban, V., 2006, Interpretation of whole-rock geochemical data in igneous geochemistry—introducing Geochemical Data Toolkit (GCDkit): Journal of Petrology, v. 47, no. 6, p. 1255–1259.

John, D.A., du Bray, E.A., Blakely, R.J., Fleck, R.J., Vikre, P.G., Box, S.E., and Moring, B.C., 2012, Miocene magmatism in the Bodie Hills volcanic field, California and Nevada—a long-lived eruptive center in the southern segment of the ancestral Cascades arc: Geosphere, v. 8, no. 1, p. 44–97.

Kerr, S.B., 1987, Petrology of Pliocene (?) basalts of Curlew Valley (Box Elder County) Utah: Logan, Utah State University, M.S. thesis, 84 p.

Langenheim, V.E., Miller, D.M., Felger, T.J., and Wells, M.L., 2011, New aeromagnetic survey reveals widespread Quaternary and Neogene volcanic rocks and footwall structure in northwest Utah: Geological Society of America Abstracts with Programs, v. 43, no. 4, p. 49.

Langenheim, V.E., Oaks, R.Q., Willis, H., Hiscock, A.I., Chuchel, B.A., Rosario, J., and Hardwick, C.L., 2014, Preliminary isostatic residual gravity map of the Tremonton 30′ x 60′ quadrangle, Box Elder and Cache Counties, Utah, and Franklin and Oneida Counties, Idaho: Utah Geological Survey Miscellaneous Publication 14-2, 4 p., 1 plate, 6 data files, scale 1:100,000, CD.

Langenheim, V.E., Willis, H., Athens, N.D., Chuchel, B.A., Kraushaar, S.M., Knepprath, N.E., Rosario, J., Roza, J., Hiscock, A.I., and Hardwick, C.L., 2013, Preliminary isostatic gravity map of the Grouse Creek and east part of the Jackpot 30′ x 60′ quadrangles, Box Elder County, Utah, and Cassia County, Idaho: Utah Geological Survey Miscellaneous Publication 13-2, 3 p., 1 plate, 4 data files, scale 1:100,000, CD.

LeBas, M.J., Le Maitre, R.W., Streckheisen, A., and Zenettin, B., 1986, A chemical classification of volcanic rocks

based on the total alkali-silica diagram: Journal of Petrology, v. 27, p. 745–750.

McCalpin, J.P., Robison, R.M., and Garr, J.D., 1992, Neotectonics of the Hansel Valley–Pocatello Valley corridor, northern Utah and southern Idaho, *in* Gori, P.L., and Hays, W.W., editors, Assessment of regional earthquake hazards and risk along the Wasatch Front, Utah: U.S. Geological Survey Professional Paper 1500, p. Gl–Gl8.

McPhie, J., Doyle, M., and Allen, R., 1993, Volcanic textures—a guide to the interpretation of textures in volcanic rocks: Centre for Ore Deposit and Exploration Studies, University of Tasmania, Hobart, 198 p.

Miller, D.M., 1997a, Interim geologic map of the Monument Peak NW quadrangle, Box Elder County, Utah and Oneida County, Idaho: Utah Geological Survey Open-File Report 345, 34 p., 1 plate, scale 1:24,000.

Miller, D.M., 1997b, Interim geologic map of the Monument Peak NE quadrangle, Box Elder County, Utah and Oneida County, Idaho: Utah Geological Survey Open-File Report 346, 34 p., 1 plate, scale 1:24,000.

Miller, D.M., 1997c, Interim geologic map of the Locomotive Springs quadrangle, Box Elder County, Utah: Utah Geological Survey Open-File Report 349, 34 p., 1 plate, scale 1:24,000.

Miller, D.M., Clark, D.L., Wells, M.L., Oviatt, C.G., Felger, T.J., Langenheim, V.E., and Todd, V.R., in preparation, Geologic map of the Grouse Creek and east part of the Jackpot 30′ x 60′ quadrangles, Box Elder County, Utah, and Cassia County, Idaho: Utah Geological Survey Map, scale 1:62,500.

Miller, D.M., Clark, D.L., Wells, M.L., Oviatt, C.G., Felger, T.J., and Todd, V.R., 2012, Progress report geologic map of the Grouse Creek 30′ x 60′ quadrangle and Utah part of the Jackpot 30′ x 60′ quadrangle, Box Elder County, Utah, and Cassia County, Idaho (year 3 of 4): Utah Geological Survey Open-File Report 598, 31 p., 1 plate, scale 1:62,500, CD.

Miller, D.M, and Felger, T.J, in preparation, Geologic map of the Tremonton 30′ x 60′ quadrangle, Box Elder and Cache Counties, Utah, and Franklin and Oneida Counties, Idaho: Utah Geological Survey Map, scale 1:100,000.

Miller, D.M., Jordan, T.E., and Allmendinger, R.W., 1990, Geologic map of the Crater Island quadrangle, Box Elder County: Utah Geological and Mineral Survey Map 128, 16 p., 2 plates, scale 1:24,000.

Miller, D.M., and Langrock, H., 1997a, Interim geologic map of the Monument Peak quadrangle, Box Elder County, Utah: Utah Geological Survey Open-File Report 344, 34 p., 1 plate, scale 1:24,000.

Miller, D.M., and Langrock, H., 1997b, Interim geologic map of the Monument Peak SW quadrangle, Box Elder County, Utah: Utah Geological Survey Open-File Report 347, 34 p., 1 plate, scale 1:24,000.

Miller, D.M., and Langrock, H., 1997c, Interim geologic map of the Monument Point quadrangle, Box Elder County, Utah: Utah Geological Survey Open-File Report 348, 34 p., 1 plate, scale 1:24,000.

Miller, D.M., Nakata, J.K., Oviatt, C.G., Nash, W.P., and Fiesinger, D.W., 1995, Pliocene and Quaternary volcanism in the northern Great Salt Lake area and inferred volcanic hazards, *in* Lund, W.R., editor, Environmental and engineering geology of the Wasatch Front region: Utah Geological Association Publication 24, p. 469–482.

Miller, D.M., Oviatt, C.G., and McGeehin, J.P., 2013, Stratigraphy and chronology of Provo shoreline deposits and lake-level implications, late Pleistocene Lake Bonneville, eastern Great Basin, USA: Boreas, v. 42, p. 342–361.

Miller, D.M., Oviatt, C.G., and Nash, B.P., 2007, Late Pleistocene Hansel Valley basaltic ash, northern Lake Bonneville, Utah, USA: Quaternary International, v. 178, p. 238–245.

Murchison, S.B., 1989, Fluctuation history of Great Salt Lake, Utah, during the last 13,000 years: Salt Lake City, University of Utah, Ph.D. dissertation, 137 p.

Oviatt, C.G., 2014, The Gilbert episode in the Great Salt Lake Basin, Utah: Utah Geological Survey Miscellaneous Publication 14-3, 20 p.

Oviatt, C.G., 2015, Chronology of Lake Bonneville, 30,000 to 10,000 yr B.P.: Quaternary Science Reviews, v. 110, p. 166–171.

Oviatt, C.G., Currey, D.R., and Miller, D.M., 1990, Age and paleoclimatic significance of the Stansbury shoreline of Lake Bonneville, eastern Great Basin: Palaeogeography, Palaeoclimatology, Palaeoecology, v. 99, p. 225–241.

Oviatt, C.G., Currey, D.R., and Sack, D., 1992, Radiocarbon chronology of Lake Bonneville, northeastern Great Basin: Palaeogeography, Palaeoclimatology, Palaeoecology, v. 99, p. 225–241.

Oviatt, C.G., and Miller, D.M., 1997, New explorations along the northern shores of Lake Bonneville: Brigham Young University Geology Studies, v. 42, part II, p. 345–371.

Oviatt, C.G., Miller, D.M., McGeehin, J.P., Zachary, C., and Mahan, S., 2005, The Younger Dryas phase of Great Salt Lake, Utah, USA: Palaeogeography, Palaeoclimatology, Palaeoecology, v. 219, p. 263–284.

Peace, F.S., 1956, History of exploration for oil and gas in Box Elder County, Utah, and vicinity, *in* Eardley, A.J., and Hardy, C.T., editors, Geology of parts of northwestern Utah: Utah Geological Society Guidebook to the Geology of Utah, No. 11, p. 17–31.

Perkins, M.E., 2014, Tephrochronology results for the Grouse Creek and east part of the Jackpot 30′ x 60′ quadrangles and vicinity, Utah, Idaho, and Nevada: Utah Geological Survey Open-File Report 630, 23 p.

Robison, R.M., and McCalpin, J.P., 1987, Surficial geology of

Hansel Valley, Box Elder County, Utah, *in* Kopp, R.S. and Cohenour, R.E., editors, Cenozoic geology of western Utah: Utah Geological Association Publication 16, p. 335–349.

Shea, R.M, 1985, Bimodal volcanism in the northeast Basin and Range—petrology of the Wildcat Hills, Utah: Salt Lake City, University of Utah, M.S. thesis, 79 p.

Smith, R.B., and Bruhn, R.L., 1984, Intraplate extensional tectonics of the eastern Basin-Range—inferences on structural style from seismic reflection data, regional tectonics, and thermo-mechanical models of brittle-ductile deformation: Journal of Geophysical Research, v. 89, p. 5733–5762.

Smith, R.B., and Sbar, M.L., 1974, Contemporary tectonics and seismicity of the western United States with emphasis on the Intermountain seismic belt: Geological Society of America Bulletin, v. 85, p. 1205–1218.

Smith, R.B., Shaw, H.R., and Ludke, R.G., 1978, Comprehensive tables giving physical data and thermal energy estimates for young igneous systems of the United States: U.S. Geological Survey Open-File Report 78-925, 15 p.

Steiger, R.H, and Jager, E., 1977, Subcommission on geochronology—convention on the use of decay constants in geo- and cosmochronology: Earth and Planetary Science Letters, v. 36, p. 359–362.

Stokes, W.L., 1963, Geologic map of northwestern Utah: Utah State Land Board, scale 1:250,000.

Todd, V.R., 1983, Late Miocene displacement of pre-Tertiary and Tertiary rocks in the Matlin Mountains, northwestern Utah, *in* Miller, D.M., Todd, V.R., and Howard, K.A., editors, Tectonic and stratigraphic studies in the eastern Great Basin: Geological Society of America Memoir 157, p. 239–270.

U.S. Geological Survey, 2015, Quaternary fault and fold database of the United States: Online, http://earthquake.usgs.gov/hazards/qfaults/.

Utah Division of Oil, Gas and Mining, 2012–2014, Well file and log databases: Online, http://oilgas.ogm.utah.gov/, accessed numerous times during 2012 through 2014.

Utah Division of Water Rights, 2014, Well drilling database: Online, http://www.waterrights.utah.gov/wellinfo/default.asp, accessed numerous times in 2014.

Walter, H.G., 1934, Hansel Valley, Utah, earthquake: The Compass of Sigma Gamma Epsilon, v. 14, no. 4, p. 178– 181.

Wells, M.L, 1992, Kinematics and timing of sequential deformations in the eastern Raft River Mountains, *in* Wilson, J.R., editor, Field guide to geologic excursions in Utah and adjacent areas of Nevada, Idaho, and Wyoming: Utah Geological Survey Miscellaneous Publication 92-13, p. 59–78.

Wells, M.L., 2009, Geologic map of the Kelton Pass quadrangle, Box Elder County, Utah, and Cassia County, Idaho: Utah Geological Survey Miscellaneous Publication 09-3, 27 p., 3 plates, scale 1:24,000 (plate 1) and 1:12,000 (plate 2), CD.

York, D., 1969, Least squares fitting of a straight line with correlated errors: Earth and Planetary Science Letters, v. 5, no. 5, p. 320–324.

Young, B., Shervais, K., Ponce-Zepeda, M., Rosove, S., and Evans, J., 2013, Hydrogeochemistry, geothermometry, and structural setting of thermal springs in northern Utah and southeastern Idaho: Utah Geological Survey Open-File Report 605, 33 p.

Zoback, M.L., 1983, Structure and Cenozoic tectonism along the Wasatch fault zone, Utah, *in* Miller, D.M., Todd, V.R., and Howard, K.A., editors, Tectonic and stratigraphic studies in the eastern Great Basin: Geological Society of America, Memoir 157, p. 3–27.

UTAH GEOLOGICAL SURVEY
a division of
Utah Department of Natural Resources
in cooperation with
U.S. Department of the Interior
U.S. Geological Survey

Plate 1
Utah Geological Survey Miscellaneous Publication 16-1DM
Geologic and Geophysical Maps and Volcanic History of the Kelton Pass SE and Monument Peak SW Quadrangles

GEOLOGIC MAP OF THE KELTON PASS SE AND MONUMENT PEAK SW QUADRANGLES, BOX ELDER COUNTY, UTAH
2016

by
Tracey J. Felger, David M. Miller, Victoria E. Langenheim, and Robert J. Fleck
U. S. Geological Survey

MAP LOCATION

SCALE 1:24,000

1 0.5 0 1 MILES

1000 0 1000 2000 3000 4000 5000 6000 7000 FEET

1 0.5 0 1 KILOMETERS

CONTOUR INTERVALS 10 AND 20 FEET
SUPPLEMENTAL CONTOUR INTERVAL 10 FEET

APPROXIMATE MEAN DECLINATION, 2016

Basemap is a mosaic of the USGS Digital Raster Graphics of the Kelton Pass SE and Monument Peak SW topographic maps.
Projection: UTM Zone 12
Datum: NAD 1983

Field mapping conducted summers of 1989 -1995 by Miller and Holly Langrock, and 2006 - 2008 by Miller and Felger

1	2	3	4
5			6
7	8	9	10

1. Kelton Pass
2. Curlew Junction
3. Monument Peak NW
4. Monument Peak NE
5. Black Butte
6. Monument Peak
7. Peplin Flats
8. Crocodile Mountain NE
9. Locomotive Springs
10. Monument Point

ADJOINING 7.5' QUADRANGLE NAMES

ISBN 978-1557919199

UTAH GEOLOGICAL SURVEY
a division of
Utah Department of Natural Resources
in cooperation with
U.S. Department of the Interior
U.S. Geological Survey

Plate 2
Utah Geological Survey Miscellaneous Publication 16-1DM
Geologic and Geophysical Maps and Volcanic History of the Kelton Pass SE and Monument Peak SW Quadrangles

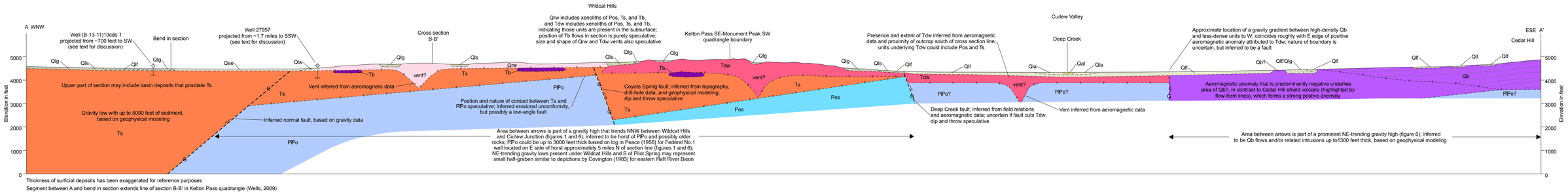

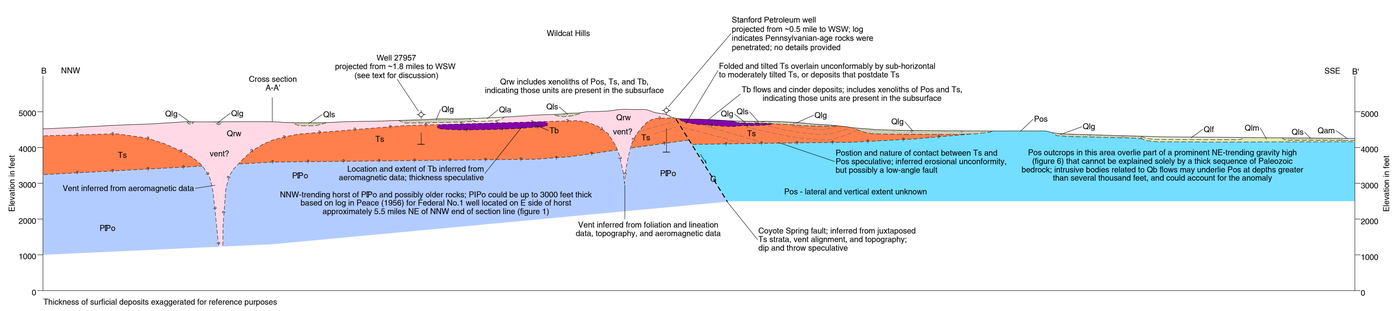

CORRELATION OF MAP UNITS

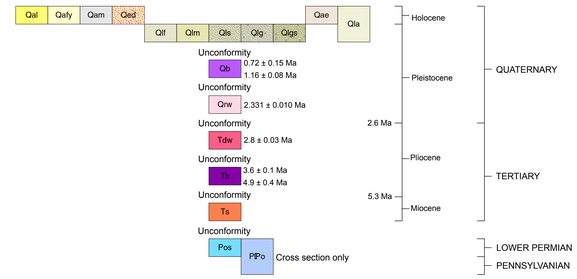

GEOLOGIC SYMBOLS

- Contact - Dashed where approximately located; queried on cross sections where speculative
- Concealed normal fault - Inferred from geophysical data (G) or other indirect methods; bar and ball on downthrown side; shown as dashed line with arrows on cross section
- Lake Bonneville shorelines - P=Provo; S=Stansbury; G=Gilbert; PV=Pilot Valley; t=transgressive
- Vegetation or topographic lineament of unknown origin
- Concealed syncline - Arrow indicates direction of plunge
- Lava flow direction
- Lava flow and bedding form lines (on cross sections only)
- A A' Line of cross section
- Sedimentary bedding attitude -
  - 20 Inclined
- Igneous foliation or lineation attitude -
  - Horizontal
  - 35 Inclined
  - Vertical
  - Flow lineation
- Planar feature of uncertain origin -
  - 20 Inclined
  - Vertical
- Paleosol location
- Volcanic vent, very approximately located
- Geochemistry sample location and number
- Geochronology sample location, number, and age (Ma)
- Fossil sample location and number
- Tephrochronology sample location and number
- Drill hole location and identifier

View westward from summit of Cedar Hill, showing the Wildcat Hills in the middle distance, and the east flank of the Raft River Mountains in the background (right side of photo). The Wildcat Hills are formed of Pleistocene rhyolite (2.331 ± 0.010 Ma) and Pliocene dacite (2.8 ± 0.03 Ma) flows that overlie Pliocene basalt (3.6 to 4.9 ma) and Miocene Salt Lake Formation.

Northwest side of Cedar Hill shield volcano. It is the largest and northernmost of three small Pleistocene shield volcanoes that erupted along the east side of Curlew Valley. Basalt flows from the summit yielded a K-Ar whole-rock age of 1.16 ± 0.08 Ma.

Lithophysae in devitrified Rhyolite of Wildcat Hills.

LIST OF MAP UNITS

QUATERNARY SURFICIAL DEPOSITS

Alluvial Deposits

- Qal Alluvium (Holocene)
- Qafy Younger alluvial-fan deposits (Holocene)
- Qam Alluvial mud (Holocene)

Eolian Deposits

- Qed Eolian sand dunes (Holocene)

Lacustrine Deposits

- Qlf Lacustrine fine-grained deposits (upper Pleistocene)
- Qlm Lacustrine marl (upper Pleistocene)
- Qls Lacustrine sand (upper Pleistocene)
- Qlg Lacustrine gravel (upper Pleistocene)
- Qlgs Lacustrine gravel and sand (upper Pleistocene)

Mixed-Environment Deposits

- Qae Mixed alluvial and eolian deposits (Holocene)
- Qla Lacustrine and alluvial deposits, undivided (Holocene and upper Pleistocene)

Stacked-Unit Deposits

- Qlf/Qlg Lacustrine fine-grained deposits over lacustrine gravel (upper Pleistocene over upper Pleistocene)
- Qlg/Tb? Lacustrine gravel over basaltic lava flows? (upper Pleistocene over Tertiary?)
- Qlgs/Ts Lacustrine gravel and sand over Salt Lake Formation (upper Pleistocene over Tertiary)
- Qlg/Pos Lacustrine gravel over Oquirrh Formation, sandstone member (upper Pleistocene over Lower Permian)

QUATERNARY AND TERTIARY VOLCANIC ROCKS

- Qb Basalt (Pleistocene)
- Qrw Rhyolite of Wildcat Hills (Pleistocene)
- Tdw Dacite of Wildcat Hills (Pliocene)
- Tb Basaltic lava flows (Pliocene)

TERTIARY SEDIMENTARY ROCKS

- Ts Salt Lake Formation, undivided (Miocene)

PERMIAN AND PENNSYLVANIAN SEDIMENTARY ROCKS

- Pos Oquirrh Formation, sandstone member (Lower Permian)
- PPo Oquirrh Formation, undivided (Lower Permian to Lower Pennsylvanian) - Cross section only